Multilocus Patterns of Nucleotide Diversity and Divergence Reveal Positive Selection at Candidate Genes Related to Cold Hardiness in Coastal Douglas Fir (*Pseudotsuga menziesii* var. *menziesii*)

Andrew J. Eckert,*,† Jill L. Wegrzyn,‡ Barnaly Pande,‡ Kathleen D. Jermstad,§
Jennifer M. Lee,* John D. Liechty,* Brandon R. Tearse,‡
Konstantin V. Krutovsky** and David B. Neale*,§,1

*Section of Evolution and Ecology, †Center for Population Biology and ‡Department of Plant Sciences, University of California, Davis,
California 95616, §Institute of Forest Genetics, Pacific Southwest Research Station, U.S. Department of Agriculture Forest Service,
Placerville, California 95667 and **Department of Ecosystem Science and Management,
Texas A&M University, College Station, Texas 77843

ABSTRACT

Forest trees exhibit remarkable adaptations to their environments. The genetic basis for phenotypic adaptation to climatic gradients has been established through a long history of common garden, provenance, and genecological studies. The identities of genes underlying these traits, however, have remained elusive and thus so have the patterns of adaptive molecular diversity in forest tree genomes. Here, we report an analysis of diversity and divergence for a set of 121 cold-hardiness candidate genes in coastal Douglas fir (*Pseudotsuga menziesii* var. *menziesii*). Application of several different tests for neutrality, including those that incorporated demographic models, revealed signatures of selection consistent with selective sweeps at three to eight loci, depending upon the severity of a bottleneck event and the method used to detect selection. Given the high levels of recombination, these candidate genes are likely to be closely linked to the target of selection if not the genes themselves. Putative homologs in Arabidopsis act primarily to stabilize the plasma membrane and protect against denaturation of proteins at freezing temperatures. These results indicate that surveys of nucleotide diversity and divergence, when framed within the context of further association mapping experiments, will come full circle with respect to their utility in the dissection of complex phenotypic traits into their genetic components.

A long history of common garden experiments has shown that forest trees are adapted phenotypically to local and regional climates (Morgenstern 1996). Latitudinal clines for phenological traits have been documented across a diverse set of temperate forest tree species ranging from Norway spruce [*Picea abies* (L.) Karst.] to European aspen (*Populus tremula* L.). The frequent nature of these patterns, as well as the high heritabilities and polygenic nature for many of these traits (Howe *et al.* 2003), suggest that forest tree genomes should be rife with signatures of positive natural selection.

Early efforts to detect these signatures using molecular markers were largely unsuccessful (McKay and Latta 2002). One of the limiting factors for these efforts was the genomic distribution, availability, and nonfunctional nature of the genetic markers that were utilized (Merkle and Adams 1987). The development

of high-throughput allele-specific marker detection for large sets of functional genes has revolutionized the search for adaptive genetic variation within conifers (González-Martínez *et al.* 2006). Surveys of nucleotide diversity across a diverse set of conifer species have highlighted common genomic attributes, such as the rapid decay of linkage disequilibrium (LD), and have documented the first tangible evidence of natural selection in forest tree genomes (Savolainen and Pyhäjärvi 2007; Eveno *et al.* 2008; Palmé *et al.* 2008, 2009).

Here, we take a candidate gene approach to the identification of genes underlying cold-hardiness phenotypes in coastal Douglas fir [*Pseudotsuga menziesii* (Mirb.) Franco var. *menziesii*]. A 40-year history of common garden experiments, provenance trials, and genecological studies has documented the genetic basis of growth, germination, and bud phenology traits, as well as the steep clines in genetic variability for those traits along environmental gradients (Campbell and Sorensen 1973; Campbell 1979; Aitken and Adams 1996, 1997; St. Clair *et al.* 2005; St. Clair 2006). The structure of these clines is consistent with the hypothesis

that diversifying selection (McKay and Latta 2002) or local selective sweeps (Slatkin and Wiehe 1998; Santiago and Caballero 2005) should characterize most of the signatures of positive natural selection in the genome of coastal Douglas fir. If this is the case, we expect to observe signatures of elevated levels of intermediate-frequency polymorphisms in the site frequency spectrum for those genes that underlie these clinal traits.

While the phenotypes involved with adaptation to cold temperatures are well known, the identities of the genes underlying these traits have remained elusive. Several quantitative trait loci (QTL) have been identified (Jermstad *et al.* 2001a,b, 2003), and a handful of candidate genes have been shown to collocate with these QTL (Wheeler *et al.* 2005). The genes underlying physiological responses to cold, however, are well known in *Arabidopsis thaliana* L. (Thomashow 1999). Similar types of genes are thought to underlie cold-hardiness related traits in conifers (Yakovlev *et al.* 2006; Holliday *et al.* 2008). An initial survey of nucleotide diversity at 18 candidate genes in coastal Douglas fir, however, found only limited departures from neutrality (Krutovsky and Neale 2005). The vast majority of candidate genes, as well as inference of demographic influences upon genomic patterns of nucleotide diversity, thus remain to be investigated.

Mounting evidence indicates that patterns of positive selection are pervasive throughout the genomes of Drosophila (Begun *et al.* 2007), Arabidopsis (Clark *et al.* 2007), and humans (Voight *et al.* 2006). Evidence on a genome scale is only beginning to emerge for conifers (Namroud *et al.* 2008). We used an expanded set of candidate genes to address three goals: (i) describe patterns of polymorphism and divergence within a set of 121 candidate genes for cold hardiness, (ii) identify those genes with patterns of polymorphism and divergence inconsistent with neutral expectations, and (iii) discuss the types and prevalence of selection across a conifer genome.

MATERIALS AND METHODS

Plant material and DNA isolation: A sample of 24 unrelated trees obtained from six regions located across Washington and Oregon was assembled as a diversity panel (supporting information, Table S1) for the discovery of single-nucleotide polymorphisms (SNPs). These regions are situated along temperature, precipitation, and genecological gradients identified previously for coastal Douglas fir in Oregon and Washington (St. Clair *et al.* 2005; St. Clair 2006). A single sample of bigcone Douglas fir [*P. macrocarpa* (Vasey) Mayr] collected from the Angeles National Forest was used as an outgroup. Total genomic DNA was isolated from haploid megagametophyte tissues dissected out from multiple open-pollinated seeds collected from each tree, using a DNeasy 96 plant kit (QIAGEN, Valencia, CA). All DNA extractions and quantifications were performed at the U.S. Department of Agriculture National Forest Genetics Laboratory (Placerville, CA).

Choice of candidate genes: Candidate genes with a putative role in conferring tolerance to cold temperatures were selected according to three criteria: (i) genes found to collocate with QTL for cold hardiness in Douglas fir (Wheeler *et al.* 2005), (ii) genes with physiological roles in cold tolerance response, and (iii) genes showing differential expression in microarray studies in *A. thaliana* L. (Lee *et al.* 2005). Standard BLAST tools were used to mine the Douglas fir expressed sequence tags (EST) collections housed at Virginia Polytechnic University (http://staff.vbi.vt.edu/estap) for orthologous sequences to selected candidate genes. Those collections represent four EST libraries, three of which are cold-hardiness libraries derived from 1-year-old seedlings subjected to fall, winter, and spring ambient air conditions in Corvallis, Oregon during 2003. A threshold of $1E-10$ was used to define homology during BLAST analyses. In total, 553 putative homologs were selected for primer design, of which 378 were able to have primers designed successfully. A total of 121 of those 378 genes were selected on the basis of diversity of function and sequence-based primer validation from a single Douglas fir sample (Table S2 and Table S3).

PCR, DNA sequencing, and sequence analysis: Sequence data for each candidate gene were obtained using standard PCR and Sanger sequencing protocols (Table S4). The Pine Alignment and SNP Identification Pipeline (PineSAP) was used to assemble, call bases for, align, and identify SNPs from the 5220 sequence reads (Wegrzyn *et al.* 2009). The final alignments for each candidate gene were generated using a minimum Phred quality score of 20 for base calls associated with SNPs. All alignments were further trimmed, edited, and validated using CodonCode Aligner v. 2.0.4 (CodonCode, Dedham, MA). Gene annotation, data summaries, and laboratory protocols are given at our website (http://dendrome.ucdavis.edu/dfgp).

SNP genotyping and linkage mapping analyses: A subset of the 933 discovered SNPs ($n = 384$) was chosen to validate polymorphism identifications made by PineSAP and to investigate the distribution of those polymorphisms across existing linkage maps of Douglas fir through the genotyping of 192 progeny from a three-generation outbred pedigree (*cf.* Jermstad *et al.* 1998) using Illumina's GoldenGate SNP genotyping platform. This high-throughput platform works well for the large and complex genomes of conifers (Pavy *et al.* 2008). Multiplexed genotyping was conducted at the DNA Technologies Core facility located at the University of California, Davis Genome Center. Signal intensities were quantified and matched to specific alleles, using the BeadStudio v 3.1.14 software (Illumina). A minimum GenCall$_{50}$ (GC$_{50}$) score of 0.20 was chosen for inclusion of SNP loci in the final data set and genotypic clusters were edited manually as needed (Eckert *et al.* 2009a).

The existing linkage maps for coastal Douglas fir are based largely on anonymous RFLP markers. Here, we used 189 fully informative RFLP markers, 3 isozyme markers, and the 77 segregating SNPs to infer a sex-averaged genetic linkage map using JoinMap v. 1.4 (Stam 1993). All SNP loci were assessed for conformity to Mendelian segregation ratios prior to linkage mapping, using goodness-of-fit χ^2-tests. We removed SNPs from the same candidate gene that mapped to <0.5 cM from each other prior to the production of the final genetic map. Generation of linkage maps within this pedigree is described in detail elsewhere (Jermstad *et al.* 1998, 2001a,b, 2003; Krutovsky *et al.* 2004). In brief, we used a LOD threshold of 4.0 to assign markers to linkage groups followed by a threshold of 0.10 to order markers within those inferred linkage groups. Recombination frequencies were converted to map distances in centimorgans, using the Kosambi mapping function. Linkage map results are deposited and freely available at

the forest tree CMAP website (http://dendrome.ucdavis.edu/cmap/; accession no. TG05).

Linkage disequilibrium analyses: LD between pairs of sites within each candidate gene and between pairs of sites in different candidate genes mapped to the same linkage group were evaluated by using DnaSP v. 4.50.3 (ROZAS *et al.* 2003). We used the squared allelic correlation coefficient (r^2) between pairs of parsimony informative sites to estimate LD. We used Fisher's exact tests to calculate *P*-values under the null hypothesis that LD estimates at least as extreme as those observed could have arisen under linkage equilibrium. The decay of LD with distance in base pairs between sites within the same candidate gene was evaluated with nonlinear regression, using the Gauss–Newton algorithm as implemented in the *nls* function of R (HILL and WEIR 1988; REMINGTON *et al.* 2001).

Population structure and historical demography: The extent of structure among populations of coastal Douglas fir observed at chloroplast and nuclear microsatellites, as well as allozymes, is low and consistent with weak effects of isolation by distance (LI and ADAMS 1989; VIARD *et al.* 2001; KRUTOVSKY *et al.* 2009). We analyzed patterns of differentiation for all 115 polymorphic candidate genes, using pairwise measures of divergence (D_{xy}) among the six populations, and related this measure to geographical distance using Mantel tests.

To assess the effects of historical demography, especially given the weak patterns of population structure, on the ability to identify candidate genes under selection, we used a likelihood-free Markov chain Monte Carlo (MCMC) approach to estimate parameters under an instantaneous growth model (IGM) (MARJORAM *et al.* 2003; MARJORAM and TAVARÉ 2006). This model is specified by two parameters, the ratio (f) of the current effective population size (N_{ec}) to the effective population size prior to the growth event (N_{ep}) and the time in units of $4N_{ec}$ generations at which the growth event began (τ). We assigned uniform priors to both parameters, used the average Tajima's *D* over the 18 loci analyzed by KRUTOVSKY and NEALE (2005) as the metric ($D = -0.248$), and specified a rejection threshold (ε) of 0.05.

Parameters were estimated with Markov chains that were run for 1.2×10^6 steps with the first 0.2×10^6 steps being discarded as burn-in and a thinning interval of 100 steps. The resulting 10,000 samples for each parameter were taken as an approximation of their unknown posterior distributions. The joint posterior distribution of *f* and τ was smoothed, using the kernel smoothing functions available in R. Convergence was assessed through three independent MCMC runs by analyzing similarities between the resulting approximate posterior distributions and using effective sample size (ESS) estimates calculated using the CODA ver. 0.13-2 package in R.

To understand the effects of more complicated demographic scenarios on our abilities to detect loci under selection, we also analyzed two bottleneck models, where we set the time of the bottleneck to occur at 10,000 (BIM_10; $\tau = 0.001$) or 100,000 (BIM_100; $\tau = 0.015$) years ago with bottleneck sizes that were 1% of the current population size. The duration of the bottleneck was set to 0.005 coalescent time units, and the estimate of Θ upon which the simulations were conditioned was adjusted so that the average simulated value of θ_π per locus was equal to the observed value for each of the 18 loci used to fit the model. Model fit was assessed by simulating 10,000 sets of 18 loci for which we calculated the average and standard deviation of Tajima's *D*. We used these simulated sets of data to differentiate among models (instantaneous growth or the two bottleneck models), using rejection sampling ($\varepsilon = 0.05$ for both *D* and the standard deviation of *D*) and the relationship between acceptance rates and Bayes factors (BF $= P(S|\text{BIM}\_i)/P(S|\text{IGM})$, where $P(S|\text{Model})$ is given by the acceptance rate and represents the probability of the observed statistics given the model). The observed values of average *D* and the standard deviation of *D* were -0.248 and 0.837, respectively (KRUTOVSKY and NEALE 2005). Following JEFFREYS (1998), we considered values $>10^{-1/2}$ for the BF as "substantial" evidence for a given model (*cf.* ROSS-IBARRA *et al.* 2009). This scheme conditions all comparisons on the estimates of τ and *f* from the instantaneous growth model (*i.e.*, these were not estimated again) given added demographic effects (*e.g.*, bottlenecks).

Nucleotide diversity and neutrality tests: Several estimators of $\Theta = 4N_e u$, where N_e is the effective population size and *u* is the mutation rate, were used to assess the magnitude of nucleotide diversity across candidate genes. A likelihood-ratio test was performed subsequently to test the null hypothesis that Θ is constant across loci (HUDSON 1991). The number of haplotypes (*h*) and haplotypic diversity (H_d) were calculated for comparison with diversity estimators based on the site frequency spectrum. Pairwise divergence (D_{xy}) for each candidate gene was calculated by comparing the sequences of coastal Douglas fir to a single sequence from bigcone Douglas-fir. We assumed for all calculations that our data conformed to the infinite-sites model. Sites violating these assumptions, or those with missing data, were ignored.

A suite of summary statistics was used to detect departures of the site frequency spectrum from neutral expectations within each candidate gene. The significance of each statistic was determined under three different null models, using 10,000 coalescent simulations conditional on the observed value of θ_π. When simulating data under the demographic models, we adjusted the value of Θ so that the median value of the simulated θ_π was equal to the observed data. This was done to account for the fact that θ_π is only an unbiased estimator of Θ under genetic drift. The positive false discovery rate (FDR) method was used to correct for multiple testing (STOREY 2003). We chose to focus on positive selection, because many of the tests we employed are most powerful in differentiating positive from background selection (ZENG *et al.* 2006, 2007a,b). We employed the DHEW test to search further for departures from neutrality. This test uses the combination of Tajima's *D*, Fay and Wu's normalized *H*, and the Ewens–Watterson test of neutrality to detect positive selection. The rejection region for this test was determined through 50,000 coalescent simulations conditional on the observed value of θ_π. We used a nominal threshold of $P = 0.0005$ in the calculation of this region for each locus to account for the fact that we are performing 115 independent tests.

Finally, we used polymorphism–divergence-based tests to search for candidate genes with reduced levels of polymorphism relative to divergence. A maximum-likelihood implementation of the Hudson–Kreitman–Aguade (HKA) test was carried out with MLHKA ver. 2.0 (WRIGHT and CHARLESWORTH 2004). We implemented a likelihood-ratio test by choosing randomly 20 candidate genes exhibiting neutral site frequency spectra and 3 candidate genes exhibiting reduced levels of polymorphism relative to divergence. These 3 genes were chosen because they had reduced levels of polymorphism relative to divergence ($\theta_\pi/D_{xy} < 0.15$). The likelihood function was evaluated and parameters were estimated under both models, using MCMC with 1.0×10^8 steps. Statistical significance was determined by comparing twice the difference between the log-likelihood scores to a χ^2-distribution with 3 d.f., where in model 1 it was assumed that all 23 loci were neutral and in model 2 it was assumed that the 3 focal genes were nonneutral. Three independent MCMC simulations were used to check for convergence of the likelihood score and parameter estimates.

We also computed the ratio of nonsynonymous (K_a) to synonymous (K_s) divergence for each gene using DnaSP and

correlated the K_a/K_s ratio to the polymorphism/divergence ratio using simple linear regression in R. This ratio is the average of each pairwise estimate of K_a/K_s of the coastal Douglas fir samples to the single bigcone Douglas fir. We used bootstrapping ($n = 10,000$ replicates) across samples to construct 95 and 99% confidence intervals for our measure of K_a/K_s.

RESULTS

Patterns of nucleotide diversity and divergence: A total of 59,173 bp of aligned sequence data, of which 932 bp had missing, ambiguous, or indel data, were generated through the partial resequencing of 121 candidate genes (GenBank accession nos. EU864545–EU867209). The average length of these gene fragments was 489 bp ($\pm$ 204 bp). These genes are distributed throughout the genome of coastal Douglas fir (Figure S1), with 64 of the 77 segregating SNPs being placed on the existing linkage map. These 64 SNPs represent 42 candidate genes, 36 from this study and 6 from Krutovsky and Neale (2005). Sequence data were obtained for 21 of the 24 samples per gene on average. Of the 121 candidate genes, 115 were polymorphic, yielding a total of 933 SNPs. The number of polymorphisms varied greatly across genes with an average of 8 SNPs per locus (range: 0–29). The majority of SNPs were silent ($n = 732$), with 478 of those being located in noncoding regions. The remaining 201 SNPs were nonsynonymous, with an average of 2 nonsynonymous SNPs per gene (range: 0–12). The average SNP density ranged from a maximum of 1 SNP per 43 bp for silent sites to a minimum of 1 SNP per 112 bp for nonsynonymous sites.

Average estimates of nucleotide diversity were on the order of 4.0×10^{-3} per site, with silent sites having the greatest ($\theta_W = 0.00777$, $\theta_\pi = 0.00756$) and nonsynonymous sites the smallest ($\theta_W = 0.00214$, $\theta_\pi = 0.00200$) average estimates of diversity (Figure 1, Table 1 and Table S5). Diversity at synonymous (θ_{π_s}) and silent ($\theta_{\pi_{sil}}$) sites was approximately fourfold greater than at nonsynonymous sites (θ_{π_a}), with most genes exhibiting a $\theta_{\pi_a}/\theta_{\pi_s}$ ratio less than one ($n = 77$). Six genes, however, had $\theta_{\pi_a}/\theta_{\pi_s}$ ratios greater than one, with values ranging from 1.13 to 3.09 (Table S2).

Nucleotide diversity was also heterogeneous across candidate genes. A likelihood-ratio test indicated that Θ significantly varied across genes when considering all sites ($\chi^2 = 156.59$, d.f. $= 114$, $P = 0.005$), with the same result occurring for different categories of sites (silent, $\chi^2 = 189.11$, d.f. $= 111$, $P < 0.001$; nonsynonymous, $\chi^2 = 95.67$, d.f. $= 71$, $P = 0.027$). In general, θ_W was larger than θ_π, illustrating an excess of rare SNP alleles relative to expectations under neutrality.

All candidate genes exhibited an excess of divergence relative to diversity, with the average divergence estimate approximately twofold greater than the average diversity estimate (Figure 1, Table 1, and Table S6). The
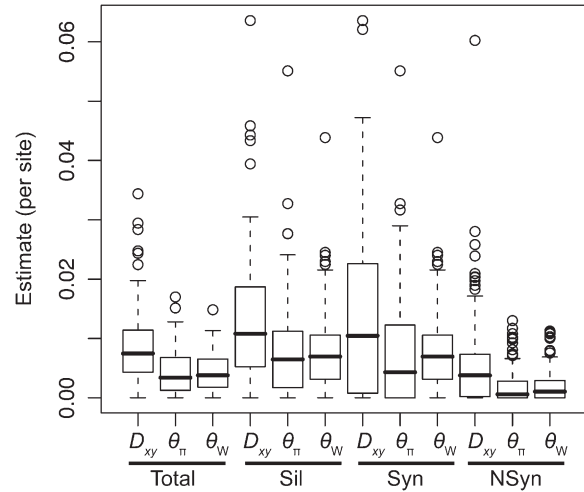
FIGURE 1.—The distribution of diversity and divergence across different categories of sites. Values are given on a per site scale. Divergence is measured against bigcone Douglas-fir. Vertical lines extend to 1.5 times the interquartile range. Syn, synonymous sites; Sil, silent sites; NSyn, nonsynonymous sites; Total, all sites.

magnitudes of divergence also differed by category of sites. Divergence at synonymous (K_s) and silent (K_{sil}) sites was greater than at nonsynonymous (K_a) sites, with 76 genes exhibiting a K_a/K_s ratio less than one or zero. However, 18 genes had a K_a/K_s ratio that was greater than one, with values ranging from 1.01 to 14.48. Two of these 18 genes had bootstrap confidence intervals excluding one (Table 1). The remaining 27 genes had undefined values for K_a/K_s.

Patterns of intra- and intergenic linkage disequilibrium: The number of haplotypes at each polymorphic locus varied from 2 ($H_d = 0.087$) to 20 ($H_d = 0.991$), with an average of 5 ($\bar{H}_d = 0.585$) per locus. The estimated minimum number of recombination events (R_M) was positively correlated with the number of haplotypes and the number of segregating sites (Kendall's $\tau > 0.409$), whereas divergence for all, silent, synonymous, and nonsynonymous sites was uncorrelated with R_M (*c.f.* Hudson and Kaplan 1985). Nucleotide diversity at synonymous and nonsynonymous sites was also uncorrelated with R_M.

The relationship of the squared allelic correlation coefficient (r^2) with physical distance illustrated that LD decayed $\sim$50% over 1100 bp, with r^2 dropping to <0.25 by 900 bp (Figure 2A). Using Fisher's exact tests, the value of r^2 for 866 of the 2837 intragenic site pairs remained significant after a Bonferroni correction. Significant intergenic LD was also apparent for candidate genes that were located proximally on linkage groups. For example, linkage group 17 has two candidate genes whose polymorphisms are almost in complete LD despite being $\sim$30 cM apart, while genes farther apart show little LD (Figure 2B).

Measures of diversity and divergence across 121 candidate genes putatively affecting cold hardiness in Douglas fir

	S	θ_W	θ_π	D_{xy}
All	**933** (8 ± 7)	**0.00450** (0.00331)	**0.00435** (0.00358)	**0.00852** (0.00619)
Silent	**732** (6 ± 6)	**0.00777** (0.00677)	**0.00756** (0.00765)	**0.01296** (0.01059)
Synonymous	**254** (2 ± 2)	**0.00791** (0.00821)	**0.00760** (0.00901)	**0.01413** (0.01498)
Nonsynonymous	**201** (2 ± 2)	**0.00214** (0.00281)	**0.00200** (0.00297)	**0.00580** (0.00806)

Values in boldface type represent totals for the number of segregating sites (S) and averages for measures of diversity (θ_W, θ_π) and divergence (D_{xy}). Numbers in parentheses are averages $\pm$ one standard deviation for S and standard deviations for θ_W, θ_π, and D_{xy}. Estimates of diversity and divergence are scaled to length of the aligned data, ignoring sites with missing data or insertion–deletion polymorphisms (indels).

Historical demography: The IGM yielded well-defined approximate posterior probability distributions for the parameters of interest. Replicated runs of the MCMC sampler converged to similar posterior probability distributions, as well as to roughly similar point estimates of the parameters (Figure S2, Table S7). Parameter estimates for this model are consistent with population growth producing a modest increase in effective population size ($f = 0.60$–0.73), beginning ~ 0.039–0.045 coalescent time units ago. These translate into minimum age estimates for the onset of growth of $\sim 270,000$–$310,000$ years ago if we assume a mutation rate on the order of 1.0×10^{-9} mutations/bp/year (WILLYARD *et al.* 2006), a generation time of 50 years, and a genomewide estimate for Θ of 5.92.

We also fit the data to two extreme bottleneck models, where the effective population size during the bottleneck was 5% of the current size (Figure 3). All other parameters were set to the mean values across the MCMC replications (Table S7). When this event was set to occur at 10,000 years ago, the Bayes factor with respect to the instantaneous growth model was 0.15. When the bottleneck, however, was set to be 100,000 years ago, the Bayes factor was 2.5. Following JEFFREYS (1998), the IGM fits the data substantially better than the BIM_10 (BF = 6.67, *i.e.*, 1/0.15), but the IGM and BIM_100 models are not differentiated substantially by the data (BF = 2.50). We focus subsequently on the two best models for the purpose of neutrality testing.

Neutrality tests: Six candidate genes exhibited clear patterns of polymorphism and divergence consistent with natural selection. The results from univariate tests are given in Table S8 and Table S9, as well as *P*-values under null models corresponding to Wright–Fisher mating, the instantaneous growth model, and the extreme bottleneck model set to occur at 100,000 years ago. On average, the summary statistics reflected the excess of low-frequency SNP alleles ($D = -0.142$) and the slight excess of high-frequency (Fay and Wu's $H = -0.106$) derived SNP alleles.

A compound test based on D, H, and the Ewens–Watterson haplotype test (DHEW) identified four genes as having patterns of diversity consistent with selective sweeps (Table 2, Figure S3). Products from all four genes function as structural components of the plasma membrane or provide protection against temperature-dependent denaturation of proteins. Inclusion of demographic models (IGM and BIM_100) into the simulations caused one of these loci (CN634517.1) to become nonsignificant.

Three genes exhibited a significant excess of divergence relative to diversity, using a maximum-likelihood implementation of the HKA test ($\chi^2 = 12.60$, d.f. = 3, $P = 0.006$). These excesses ranged from a two- to threefold reduction in diversity relative to divergence (Table S10, Figure S3), which was also apparent across different categories of sites (Figure S4). All three loci function in generalized stress responses at the levels of protein folding and transcriptional regulation, with locus Pm_CL908Contig1 also being significant for the DHEW test. A weak, yet statistically significant, relationship also existed between K_a/K_s and θ_π/D_{xy} ($F_{1,91} = 4.79$, $P = 0.031$, $r^2 = 0.05$). The driver behind this result was three loci with extreme values of K_a/K_s (*i.e.*, >5, *cf.* Table 1), all of which had $\theta_\pi/D_{xy} < 0.15$ (Table 2). Removal of these three loci changed the relationship to be nonsignificant.

Several additional genes exhibited patterns of polymorphism consistent with balancing or diversifying selection, depending upon the null model and summary statistic that was used (Table S8 and Table S9). None of these were significant using the DHEW test. For three of these five genes, a significant and positive relationship existed between geographical distance and pairwise D_{xy} among populations (Figure S5). This pattern is suggestive of diversifying selection along environmental gradients, especially given that only five candidate genes had a significant value of Mantel's r and three of those five had positive values of D that were nominally significant. Two of these genes remained significant at the FDR threshold of $Q = 0.10$ for Tajima's test when an extreme bottleneck was included as part of the null model. These loci, CN636901.1 and Pm_CL1400Contig1, encode proteins that are involved with abiotic stress response and cell wall architecture, respectively.
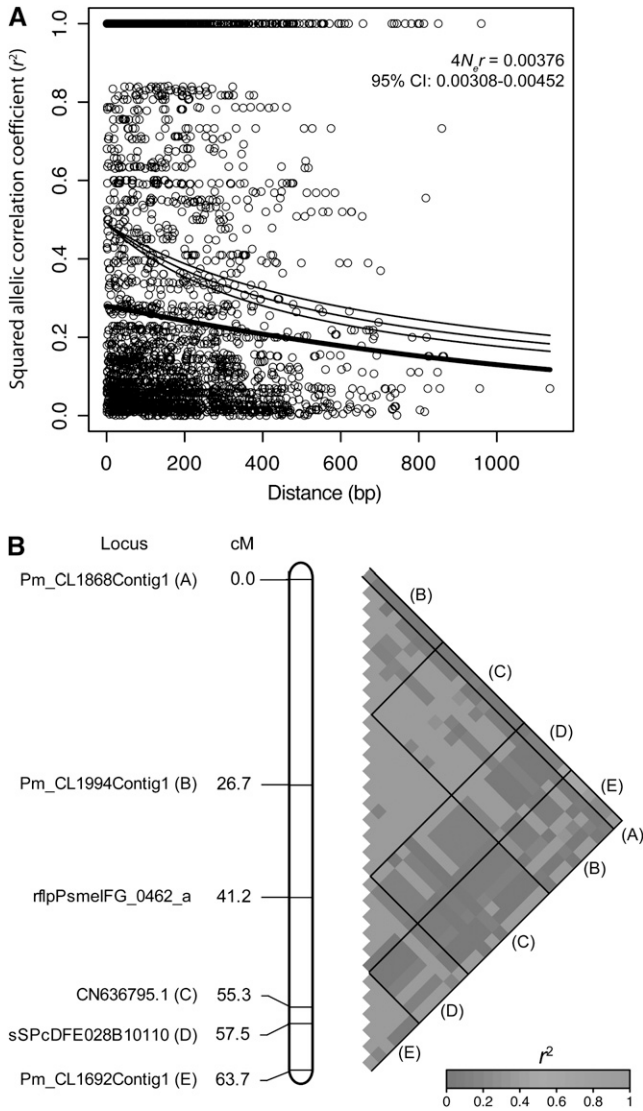
FIGURE 2.—Patterns of intra- and interlocus linkage disequilibrium (LD) for coastal Douglas fir. (A) Intragenic patterns of LD using only parsimony informative sites. The fitted lines are the expectation of r^2 (plus a 95% confidence interval for C), using the nonlinear least squares estimate of $C = 4N_e r$, where N_e is the effective population size and r is the recombination rate. The thick line is that given for the decay of LD in a previous study of coastal Douglas fir (KRUTOVSKY and NEALE 2005). (B) Patterns of intergenic LD along linkage group 17. Solid lines delineate comparisons within and among candidate genes, with letters indicating placement of the candidate genes within the matrix.

DISCUSSION

Nucleotide diversity and linkage disequilibrium: Nucleotide diversity in coastal Douglas fir is similar to, but slightly higher than, that observed in other conifer species (SAVOLAINEN and PYHÄJÄRVI 2007). The average nucleotide diversities for all, silent, and nonsynonymous sites were similar to those reported previously (KRUTOVSKY and NEALE 2005). Magnitudes of intragenic LD were moderate as compared to those reported for

conifers. Our estimate of recombination ($\rho/\Theta = 0.86$) was similar to that reported in loblolly pine ($\rho/\Theta = 0.29$; BROWN *et al.* 2004), but almost an order of magnitude less than that reported in Norway spruce ($\rho/\Theta = 1.23$–4.05; HEUERTZ *et al.* 2006) and the central populations of Scots pine ($\rho/\Theta = 3.80$–5.80; PYHÄJÄRVI *et al.* 2007).

Interlocus LD was higher than expected on the basis of results from loblolly pine and the previous study in coastal Douglas fir (BROWN *et al.* 2004; KRUTOVSKY and NEALE 2005). While genomic variation in recombination rates has been documented across plants (GAUT *et al.* 2007), which could reflect repetitive regions of the genome where recombination is suppressed, several additional processes such as natural selection, mutation rate variation, population structure, and extreme bottlenecks can also account for these patterns. This is important given that interlocus LD has dramatic effects on the amount and pattern of genetic diversity and population differentiation, as well as on the response to and efficacy of natural selection, across the genome of an organism (LE CORRE and KREMER 2003).

Patterns of selection: Most genes exhibited an excess of nucleotide diversity at synonymous relative to nonsynonymous sites, suggesting the widespread occurrence of purifying selection in coastal Douglas fir (*cf.* PALMÉ *et al.* 2009). Values of Tajima's *D* across different categories of sites were consistent with this pattern as well (Figure S6). These patterns have been noted extensively in forest trees and have driven the hypothesis that detectable patterns of positive selection in conifers are rare. This hypothesis has been confirmed in a recent examination of genomewide patterns of population differentiation in white spruce (NAMROUD *et al.* 2008; but see EVENO *et al.* 2008). Further examination using phylogenetic approaches, however, has detected patterns consistent with directional selection (PALMÉ *et al.* 2008, 2009), suggesting that consideration of relevant timescales is important to the search for selection.

We concur with this hypothesis showing that ~5% of the genes exhibited patterns consistent with positive selection. Our estimate is likely to be a lower bound due to low statistical power and the conservative assumptions that we made, as well as to the fact that causal variants may exhibit patterns of polymorphism that are indistinguishable from neutral variants due strictly to the quantitative genetic mechanisms underlying the trait (LE CORRE and KREMER 2003). Also of consideration are other models of selective sweeps incorporating selection on a standing crop of neutral variants (*cf.* INNAN and KIM 2004). In those models, linked neutral variants are less likely to show the traditional signs of selective sweeps. Contrary to expectations based on patterns of low levels of intragenic LD, the strongest signals came from those genes where patterns were consistent with selective sweeps. The vast majority of candidate genes showed little evidence of elevated levels of
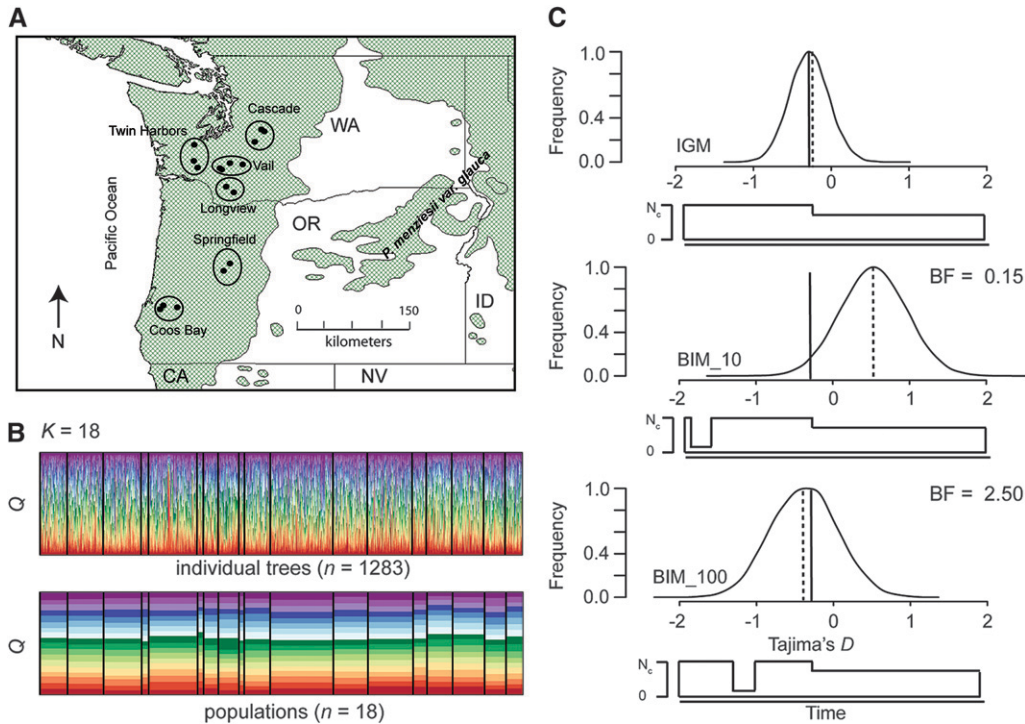
FIGURE 3.—The distribution of and historical demographic inferences for coastal Douglas fir. (A) The distribution of coastal Douglas fir in Oregon and Washington. Locations for samples are indicated with solid circles and grouped into local populations. (B) Patterns of population structure in coastal Douglas fir. Data and results are from KRUTOVSKY *et al.* (2009), who used 1283 samples and 31 allozyme and microsatellite loci. Illustrated is the smallest value of K judged as optimal using the ΔK method (EVANNO *et al.* 2005) for categories corresponding to individuals (top) and populations (bottom). (C) Demographic inferences for coastal Douglas fir. The solid line represents the average value of Tajima's D across the 18 loci used to fit the model (*cf.* KRUTOVSKY and NEALE 2005), whereas the dashed line denotes the mean of the simulated distribution under each model (IGM, instantaneous growth model; BIM_10, bottleneck 10,000 years ago; BIM_100, bottleneck model 100,000 years ago). Listed for the BIM models are Bayes factors relative to the IGM.

intermediate-frequency SNP alleles as expected under diversifying selection and recurrent selective sweep models. Under the bottleneck scenarios, however, two genes had significantly positive values of Tajima's D.

It is likely that these patterns represent relatively recent and single, not recurrent, selective sweep events. A genomewide phenomenon of recurrent selective sweeps would produce average values of D and H that were negative and positive, respectively (PRZEWORSKI 2002). Our genes, however, are not random genomic samples, and 42 of the 121 candidate genes exhibit this predicted pattern, producing average values of $D = -0.83$ and $H = 0.55$. A conclusion to rule out all occurrences of recurrent sweep models (GILLESPIE 2001) within conifer genomes, therefore, is premature, especially given our ignorance about large-scale genomic patterns of LD, the spatial distribution of genes across chromosomes, and the historical demography of these lineages.

The simplicity of our demographic models may not account for all of the confounding effects of demography on tests for selection. It also is possible that we have missed evidence supportive of other demographic models due to our limited sampling with respect to the range of coastal Douglas fir. Expansion from bottlenecks could produce patterns consistent with signatures of single and recurrent selective sweeps, depending on the timing and severity of the bottleneck. This is the most common form of demographic model fitted to

European forest trees (HEUERTZ *et al.* 2006; PYHÄJÄRVI *et al.* 2007). The severity of the bottleneck would have to be extreme to produce genomewide patterns mirroring single selective sweeps. Incorporation of an extreme bottleneck (99% reduction of N_{ec}) occurring 100,000 years ago into the null model caused one of the four genes significant previously in the DHEW test to become nonsignificant. It remains significant, however, at a nominal threshold of $P = 0.001$.

Paleobotanical and geological evidence indicate that Pleistocene glaciation in North America differed dramatically from that in Europe, making an extreme bottleneck model unlikely for coastal Douglas fir. The spatial extent of continental glaciers was smaller and vegetation was not compressed to the same degree, especially on the west coast (GRAHAM 1999). The most parsimonious demographic model for coastal Douglas fir is one of population expansion. Inclusion of a bottleneck following the instantaneous expansion, however, did provide a marginally better fit to the data (Figure 3). The data used to test the demographic models did not have outgroup information, and further work, therefore, should examine rigorously a broad range of demographic models (*cf.* INGVARSSON 2008).

Putative targets of selection: The most significant departures from neutrality came from genes that encoded proteins that are structural components of or associated with cellular membranes or those that function as or regulate chaperones. Locus Pm_CL908Contig1 con-

<div align="center">

TABLE 2

A list of candidate genes putatively affected by positive natural selection

</div>

Locus	Gene product	Result[a]
Compound *DHEW* test		
Pm_CL908Contig1	GRAM-containing/ABA-responsive protein	$P_D = 0.001$, $P_H < 0.001$, $P_{EW} = 0.080$
ES420171.1	Cold-regulated plasma membrane protein	$P_D = 0.009$, $P_H = 0.050$, $P_{EW} = 0.035$
ES420250.1	Dehydrin-like protein	$P_D = 0.072$, $P_H = 0.083$, $P_{EW} = 0.042$
CN634517.1	Lumenal binding protein	$P_D = 0.034$, $P_H = 0.148$, $P_{EW} = 0.076$
Polymorphism-to-divergence		
Pm_CL61Contig1	Cyclosporin A-binding protein	$k = 0.32$
Pm_CL908Contig1	GRAM-containing/ABA-responsive protein	$k = 0.58$
CN638556.1	Transcription regulation protein	$k = 0.41$
Synonymous-to-nonsynonymous divergence		
Pm_CL922Contig1	Thaumatin-like protein	$K_a/K_s = 14.48^{**}$, $\theta_\pi/D_{xy} = 0.087$
CN634677.1	LRR receptor-like protein kinase	$K_a/K_s = 10.78^{*}$, $\theta_\pi/D_{xy} = 0.066$

[a] Results for the DHEW test are given as *P*-values (*P*) for each of the component tests (*D*, Tajima's *D*; *H*, Fay and Wu's *H*; EW, Ewens–Watterson test) comprising the joint test. Values for the EW test are one minus the left tailed probabilities (*cf.* Zeng *et al.* 2007b). Listed are *P*-values for drift within a constant size population. Loci significant when demographic models are in included in the simulations are in boldface type. For polymorphism-to-divergence tests, parameter estimates for a maximum-likelihood implementation of the HKA test are listed. Estimates of *k* are from a nested model where all three putative targets of selection are allowed to have free parameters. The parameter *k* specifies the level of elevation ($k > 1$) or reduction ($k < 1$) in diversity relative to divergence. Asterisks denote significance differences from 1.0 for the K_a/K_s ratio using bootstrapping. **$P < 0.01$, *$P < 0.05$ (*cf.* materials and methods).

tains a GRAM domain, which characterizes membrane-associated proteins such as glucosyltransferases (Doerks *et al.* 2000; Caro *et al.* 2007). The Arabidopsis homolog of locus ES420171.1 is a multispanning G-protein coupled receptor that stabilizes the plasma membrane in response to freezing temperatures (Breton *et al.* 2003). Both CN634517.1 and Pm_CL61Contig1 have homologs whose primary functions are to act as or in the regulation of chaperones (Romano *et al.* 2004). Locus Pm_CL922Contig1 encodes a thaumatin-like protein, whose homolog in Arabidopsis has gene expression induced by fungal infection (Hu and Reddy 1997). While the link between cold hardiness and disease resistance is speculative, it is tempting to correlate overall health with the ability to grow and tolerate cold efficiently. Several of these genes are also responsive to abscisic acid (ABA). Controversy has surrounded the role of ABA during cold acclimation in Arabidopsis, however, due to its general effect on plant growth in response to stress (Gilmour and Thomashow 1991).

Limitations and implications: There are several limitations to our analyses. We used a single sequence from a recently diverged outgroup so that misspecification of ancestral states is possible. This would reduce greatly the power of the HKA test employed here and significantly affect estimation of *H* (*cf.* Baudry and Depaulis 2003). This also justifies our avoidance of McDonald–Kreitman-type analyses. Background selection could have produced signatures of selective sweeps, but not with respect to *H* (Hudson and Kaplan 1995). Finally, we did not incorporate effects of population structure into our hypothesis testing. The effects of undetected structure on inference of selection from summary statistics are tied closely to sampling design and the strength of substructure (Przeworski 2002; Städler *et al.* 2009), and thus conclusions regarding the conservative or liberal nature of our estimates are premature.

Selective sweeps, while not likely the dominant type of selection across the genome of coastal Douglas fir, are nevertheless important. Here, we have identified several genes whose patterns of diversity and divergence are inconsistent with the standard neutral model, as well as simple demographic scenarios involving instantaneous growth and bottlenecks. Depending upon demographic assumptions, we have identified three to eight such loci. These genes are prime targets for further association genetic (*cf.* Eckert *et al.* 2009b) and functional studies, thus beginning to bring molecular population and quantitative genetic approaches full circle with respect to the dissection of complex traits.

LITERATURE CITED

Aitken, S. N., and W. T. Adams, 1996 Genetics of fall and winter cold hardiness of coastal Douglas-fir in Oregon. Can. J. For. Res. **26:** 1828–1837.

Aitken, S. N., and W. T. Adams, 1997 Cold hardiness under strong genetic control in Oregon populations of Pseudotsuga menziesii var. menziesii. Can. J. For. Res. **27:** 1773–1780.

BAUDRY, E., and F. DEPAULIS, 2003 Effect of misoriented sites on neutrality tests with outgroup. Genetics **165:** 1619–1622.

BEGUN, D. J., A. K. HOLLOWAY, K. STEVENS, L. W. HILLIER, Y.-P. POH *et al.*, 2007 Population genomics: whole-genome analysis of polymorphism and divergence in *Drosophila simulans*. PLoS Biol. **5:** e310.

BRETON, G., J. DANYLUK, J. B. F. CHARRON and F. SARHAN, 2003 Expression profiling and bioinformatic analyses of a novel stress-regulated multispanning transmembrane protein family from cereals and Arabidopsis. Plant Physiol. **132:** 64–74.

BROWN, G. R., G. P. GILL, R. J. KUNTZ, C. H. LANGLEY and D. B. NEALE, 2004 Nucleotide diversity and linkage disequilibrium in loblolly pine. Proc. Natl. Acad. Sci. USA **101:** 15255–15260.

CAMPBELL, R. K., 1979 Genecology of Douglas-fir in a watershed in the Oregon Cascades. Ecology **60:** 1036–1050.

CAMPBELL, R. K., and F. C. SORENSEN, 1973 Cold acclimation in seedling Douglas-fir related to phenology and provenance. Ecology **54:** 1148–1151.

CARO, E., M. M. CASTELLANO and C. GUTIERREZ, 2007 A chromatin link that couples cell division to root epidermis patterning in Arabidopsis. Nature **447:** 213–217.

CLARK, R. M., G. SCHWEIKERT, C. TOOMAJIAN, S. OSSOWSKI, G. ZELLER *et al.*, 2007 Common sequence polymorphisms shaping genetic diversity in Arabidopsis thaliana. Science **317:** 338–342.

DOERKS, T., M. STRAUSS, M. BRENDEL and P. BORK, 2000 GRAM, a novel domain in glucosyltransferases, myotubularins and other putative membrane-associated proteins. Trends Biochem. Sci. **25:** 483–485.

ECKERT, A. J., B. PANDE, E. S. ERSOZ, M. H. WRIGHT, V. K. RASHBROOK *et al.*, 2009a High-throughput genotyping and mapping of single nucleotide polymorphisms in loblolly pine (*Pinus taeda* L.). Tree Genet. Genomes **5:** 225–234.

ECKERT, A. J., A. D. BOWER, J. L. WEGRZYN, B. PANDE, K. D. JERMSTAD *et al.*, 2009b Association genetics of coastal Douglas-fir (Pseudotsuga menziesii var. menziesii, Pinaceae) I. Cold-hardiness related traits. Genetics **182:** 1289–1302.

EVANNO, G., S. REGNAUT and J. GOUDET, 2005 Detecting the number of clusters of individuals using the software STRUCTURE: a simulation study. Mol. Ecol. **14:** 2611–2620.

EVENO, E., C. COLLADA, M. A. GUEVARA, V. LÉGER, A. SOTO *et al.*, 2008 Contrasting patterns of selection at Pinus pinaster Ait. drought stress candidate genes as revealed by genetic differentiation analyses. Mol. Biol. Evol. **25:** 417–437.

GAUT, B. S., S. I. WRIGHT, C. RIZZON, J. DVORAK and L. K. ANDERSON, 2007 Recombination: an underappreciated factor in the evolution of plant genomes. Nat. Rev. Genet. **8:** 77–84.

GILLESPIE, J. H., 2001 Is the population size of a species relevant to its evolution? Evolution **55:** 2161–2169.

GILMOUR, S. J., and M. F. THOMASHOW, 1991 Cold acclimation and cold-regulated gene expression in ABA mutants of *Arabidopsis thaliana*. Plant Mol. Biol. **17:** 1233–1240.

GONZÁLEZ-MARTÍNEZ, S. C., K. V. KRUTOVSKY and D. B. NEALE, 2006 Forest tree population genomics and adaptive evolution. New Phytol. **170:** 227–238.

GRAHAM, A., 1999 *Late Cretaceous and Cenozoic History of North American Vegetation*. Oxford University Press, New York.

HEUERTZ, M., E. DE PAOLI, T. KÄLLMAN, H. LARSSON, I. JURMAN *et al.*, 2006 Multilocus patterns of nucleotide diversity, linkage disequilibrium and demographic history of Norway spruce [*Picea abies* (L.) Karst]. Genetics **174:** 2095–2105.

HILL, W. G., and B. S. WEIR, 1988 Variances and covariances of squared linkage disequilibria in finite populations. Theor. Popul. Biol. **33:** 54–78.

HOLLIDAY, J. A., S. RALPH, R. WHITE, J. BOHLMANN and S. N. AITKEN, 2008 Global monitoring of gene expression during autumn cold acclimation among rangewide populations of Sitka spruce [*Picea sitchensis* (Bong.) Carr.]. New Phytol. **178:** 103–122.

HOWE, G. T., S. N. AITKEN, D. B. NEALE, K. D. JERMSTAD, N. C. WHEELER *et al.*, 2003 From genotype to phenotype: unraveling the complexities of cold adaptation in forest trees. Can. J. Bot. **81:** 1247–1266.

HU, X., and A. S. REDDY, 1997 Cloning and expression of a PR5-like protein from Arabidopsis: inhibition of fungal growth by bacterially expressed protein. Plant Mol. Biol. **34:** 949–959.

HUDSON, R. R., 1991 Gene genealogies and the coalescent process. Oxf. Surv. Evol. Biol. **7:** 1–44.

HUDSON, R. R., and N. L. KAPLAN, 1985 Statistical properties of the number of recombination events in the history of a sample of DNA sequences. Genetics **111:** 147–164.

HUDSON, R. R., and N. L. KAPLAN, 1995 The coalescent process and background selection. Philos. Trans. R. Soc. Lond. B Biol. Sci. **349:** 19–23.

INGVARSSON, P., 2008 Multilocus patterns of nucleotide polymorphism and the demographic history of *Populus tremula*. Genetics **180:** 329–340.

INNAN, H., and Y. KIM, 2004 Pattern of polymorphism after strong artificial selection in a domestication event. Proc. Natl. Acad. Sci. USA **101:** 10667–10672.

JEFFREYS, H., 1998 *Theory of Probability*. Oxford University Press, Oxford.

JERMSTAD, K. D., D. L. BASSONI, N. C. WHEELER and D. B. NEALE, 1998 A sex-averaged linkage map in coastal Douglas-fir (*Pseudotsuga menziesii* [Mirb.] Franco) based on RFLP and RAPD markers. Theor. Appl. Genet. **97:** 762–770.

JERMSTAD, K. D., D. L. BASSONI, K. S. JECH, N. C. WHEELER and D. B. NEALE, 2001a Mapping of quantitative trait loci controlling adaptive traits in coastal Douglas-fir. I. Timing of vegetative bud flush. Theor. Appl. Genet. **102:** 1142–1151.

JERMSTAD, K. D., D. L. BASSONI, N. C. WHEELER, T. S. ANEKONDA, S. N. AITKEN *et al.*, 2001b Mapping of quantitative trait loci controlling adaptive traits in coastal Douglas-fir. II. Spring and fall cold-hardiness. Theor. Appl. Genet. **102:** 1152–1158.

JERMSTAD, K. D., D. L. BASSONI, K. S. JECH, G. A. RITCHIE, N. C. WHEELER *et al.*, 2003 Mapping of quantitative trait loci controlling adaptive traits in coastal Douglas-fir. III. Quantitative trait loci-by-environment interactions. Genetics **165:** 1489–1506.

KRUTOVSKY, K.V., and D. B. NEALE, 2005 Nucleotide diversity and linkage disequilibrium in cold–hardiness and wood-quality related candidate genes in Douglas-fir. Genetics **171:** 2029–2041.

KRUTOVSKY, K. V., M. TROGGIO, G. R. BROWN, K. D. JERMSTAD and D. B. NEALE, 2004 Comparative mapping in the Pinaceae. Genetics **168:** 447–461.

KRUTOVSKY, K. V., J. B. ST. CLAIR, R. SAICH, V. D. HIPKINS and D. B. NEALE, 2009 Estimation of population structure in coastal Douglas-fir [*Pseudotsuga menziesii* (Mirb.) Franco var. *menziesii*] using allozyme and microsatellite markers. Tree Genet. Genomes (in press).

LE CORRE, V., and A. KREMER, 2003 Genetic variability at neutral markers, quantitative trait loci and trait in a subdivided population under selection. Genetics **164:** 1205–1219.

LEE, B.-H., D. A. HENDERSON and J.-K. ZHU, 2005 The Arabidopsis cold-responsive transcriptome and its regulation by ICE1. Plant Cell **17:** 3155–3175.

LI, P., and W. T. ADAMS, 1989 Range-wide patterns of allozyme variation in Douglas-fir (*Pseudotsuga menziesii*). Can. J. For. Res. **19:** 149–161.

MARJORAM, P., and S. TAVARE, 2006 Modern computational approaches for analyzing molecular genetic variation data. Nat. Rev. Genet. **7:** 759–770.

MARJORAM, P., J. MOLITOR, V. PLAGNOL and S. TAVARÉ, 2003 Markov chain Monte Carlo without likelihoods. Proc. Natl. Acad. Sci. USA **100:** 15324–15328.

McKAY, J. K., and R. G. LATTA, 2002 Adaptive population divergence: markers, QTL and traits. Trends Ecol. Evol. **17:** 285–291.

MERKLE, S. A., and W. T. ADAMS, 1987 Patterns of allozyme variation within and among Douglas-fir breeding zones in southwest Oregon. Can. J. For. Res. **17:** 402–407.

MORGENSTERN, E. K., 1996 *Geographic Variation in Forest Trees*. UBC Press, Vancouver, British Columbia, Canada.

NAMROUD, M.-C., J. BEAULIEU, N. JUGE, J. LAROCHE and J. BOUSQUET, 2008 Scanning the genome for gene single nucleotide polymorphisms involved in adaptive population differentiation in white spruce. Mol. Ecol. **17:** 3599–3613.

PALMÉ, A. E., M. WRIGHT and O. SAVOLAINEN, 2008 Patterns of divergence among conifer ESTs and polymorphism in *Pinus sylvestris* identify putative selective sweeps. Mol. Biol. Evol. **25:** 2567–2577.

PALMÉ, A. E., T. PYHÄJÄRVI, W. WACHOWIAK and O. SAVOLAINEN, 2009 Selection on nuclear genes in a Pinus phylogeny. Mol. Biol. Evol. **26:** 893–905.

PAVY, N., B. PELGAS, S. BEAUSEIGLE, S. BLAIS, F. GAGNON *et al.*, 2008 Enhancing genetic mapping of complex genomes through

the design of highly-multiplexed SNP arrays: application to the large and unsequenced genomes of white and black spruce. BMC Genomics **9:** 21.

PRZEWORSKI, M., 2002 The signature of positive selection at randomly chosen loci. Genetics **160:** 1179–1189.

PYHÄJÄRVI, T., M. R. GARCÍA-GIL, T. KNÜRR, M. MIKKONEN, W. WACHOWIAK *et al.*, 2007 Demographic history has influenced nucleotide diversity in European *Pinus sylvestris* populations. Genetics **177:** 1713–1724.

REMINGTON, D. L., J. M. THORNSBERRY, Y. MATSUOKA, L. M. WILSON, S. R. WHITT *et al.*, 2001 Structure of linkage disequilibrium and phenotypic associations in the maize genome. Proc. Natl. Acad. Sci. USA **98:** 11479–11484.

ROMANO, P. G. N., P. HORTON and J. E. GRAY, 2004 The Arabidopsis cyclophilin gene family. Plant Physiol. **134:** 1268–1282.

ROSS-IBARRA, J., M. TENAILLON and B. S. GAUT, 2009 Historical divergence and gene flow in the genus Zea. Genetics **181:** 1399–1413.

ROZAS, J., J. C. SÁNCHEZ-DELBARRIO, X. MESSEGYER and R. ROZAS, 2003 DnaSP, DNA polymorphism analyses by the coalescent and other methods. Bioinformatics **19:** 2496–2497.

SANTIAGO, E., and A. CABALLERO, 2005 Variation after a selective sweep in a subdivided population. Genetics **169:** 485–488.

SAVOLAINEN, O., and T. PYHÄJÄRVI, 2007 Genomic diversity in forest trees. Curr. Opin. Plant Biol. **10:** 162–167.

SLATKIN, M., and T. WIEHE, 1998 Genetic hitch-hiking in a subdivided population. Genet. Res. **71:** 155–160.

ST. CLAIR, J. B., 2006 Genetic variation in fall cold hardiness in coastal Douglas-fir in western Oregon and Washington. Can. J. Bot. **84:** 1110–1181.

ST. CLAIR, J. B., N. L. MANDEL and K. W. VANCE-BORLAND, 2005 Genecology of Douglas-fir in western Oregon and Washington. Ann. Bot. **96:** 1199–1214.

STÄDLER, T., B. HAUBOLD, C. MERINO, W. STEPHAN and P. PFAFFELHUBER, 2009 The impact of sampling schemes on the site frequency spectrum in nonequilibrium subdivided populations. Genetics **182:** 205–216.

STAM, P., 1993 Construction of integrated genetic linkage maps by means of a new computer package: JoinMap. Plant J. **3:** 739–744.

STOREY, J. D., 2003 The positive false discovery rate: a Bayesian interpretation and the q-value. Ann. Stat. **31:** 2013–2035.

THOMASHOW, M. F., 1999 Plant cold acclimation: freezing tolerance genes and regulatory mechanisms. Annu. Rev. Plant Physiol. Plant Mol. Biol. **50:** 571–599.

VIARD, F., Y. A. EL-KASSABY and K. RITLAND, 2001 Diversity and genetic structure in populations of *Pseudotsuga menziesii* (Pinaceae) at chloroplast microsatellite loci. Genome **44:** 336–344.

VOIGHT, B. F., S. KUDARAVALLI, X. WEN and J. K. PRITCHARD, 2006 A map of recent positive selection in the human genome. PLoS Biol. **4:** e72.

WEGRZYN, J. L., J. M. LEE, J. D. LIECHTY and D. B. NEALE, 2009 PineSAP–Pine alignment and SNP Identification Pipeline. Bioinformatics (in press).

WHEELER, N. C., K. D. JERMSTAD, K. V. KRUTOVSKY, S. N. AITKEN, G. T. HOWE *et al.*, 2005 Mapping of quantitative trait loci controlling adaptive traits in coastal Douglas-fir. IV. Cold-hardiness QTL verification and candidate gene mapping. Mol. Breed. **15:** 145–156.

WILLYARD, A., J. SYRING, D. S. GERNANDT, A. LISTON and R. CRONN, 2006 Fossil calibration of molecular divergence infers a moderate mutation rate and recent radiations for Pinus. Mol. Biol. Evol. **24:** 90–101.

WRIGHT, S. I., and B. CHARLESWORTH, 2004 The HKA test revisited: a maximum likelihood ratio test of the standard neutral model. Genetics **168:** 1071–1076.

YAKOVLEV, I. A., C.-G. FOSSDAL, Ø. JOHNSON, O. JUNTTLIA and T. SKRØPPA, 2006 Analysis of gene expression during bud burst initiation in Norway spruce via ESTs from subtracted cDNA libraries. Tree Genet. Genomes **2:** 39–52.

ZENG, K., Y. X. FU, S. SHI and C.-I. WU, 2006 Statistical tests for detecting positive selection by utilizing high-frequency variants. Genetics **174:** 1431–1439.

ZENG, K., S. MANO, S. SHI and C.-I. WU, 2007a Comparisons of site- and haplotype-frequency methods for detecting positive selection. Mol. Biol. Evol. **24:** 1562–1574.

ZENG, K., S. SUHUA and C.-I. WU, 2007b Compound tests for the detection of hitchhiking under positive selection. Mol. Biol. Evol. **24:** 1898–1908.

GENETICS

Multilocus Patterns of Nucleotide Diversity and Divergence Reveal Positive Selection at Candidate Genes Related to Cold Hardiness in Coastal Douglas Fir (*Pseudotsuga menziesii* var. *menziesii*)

Andrew J. Eckert, Jill L. Wegrzyn, Barnaly Pande, Kathleen D. Jermstad,
Jennifer M. Lee, John D. Liechty, Brandon R. Tearse, Konstantin V. Krutovsky
and David B. Neale

TABLE S1

A list of sample identifiers and geographic locations for the coastal Douglas-fir trees comprising the diversity panel that was used to discover single nucleotide polymorphisms (SNPs) within 121 candidate genes putatively associated with cold-hardiness phenotypes.

Population	Population id	Sample ID	Latitude (°N)	Longitude (°W)
Coastal Douglas-fir				
Cascade	22	22-1	47.3302	-121.4303
		22-2	47.3500	-121.4550
		22-3	47.3302	-121.4303
		22-4	47.1225	-121.5616
		22-5	47.1225	-121.5616
Vail	24	24-1	46.4310	-122.5357
		24-2	46.5020	-122.0951
		24-3	46.4310	-122.5357
		24-4	46.5009	-122.4310
Twin Harbors	26	26-1	46.1453	-122.4837
		26-2	46.0925	-122.3437
		26-3	46.1453	-122.4842
		26-4	46.1453	-122.4842
Longview	28	28-1	46.5605	-123.2259
		28-2	47.0306	-123.2000
		28-3	46.5555	-123.2235
		28-4	46.3913	-123.1630
Springfield	30	30-1	44.2721	-122.2705
		30-2	44.0555	-122.3722
		30-3	44.0555	-122.3722
		30-4	44.2721	-122.2721
Coos Bay	32	32-1	43.2151	-124.0418
		32-2	43.2151	-124.0418
		32-3	43.2415	-124.0010
Bigcone Douglas-fir		32-4	43.2405	-123.5951
Angeles NF	na	06019	na	na

TABLE S2

Annotation for the 121 candidate genes resequenced for coastal Douglas-fir

Locus	Organism	tBLASTx	Accession	Gene Product
CD028057.1	*Oryza sativa*	7.00E-76	NM_001050147	calcium-dependent protein kinase
CN634517.1	*Pseudotsuga menziesii*	2.00E-65	Z49764	lumenal binding protein
CN634677.1	*Arabidopsis thaliana*	4.00E-50	NM_111157	LRR receptor-like protein kinase
CN635137.1	*Picea mariana*	1.00E-57	AF051202	aquaporin
CN635490.1	*Arabidopsis thaliana*	3.00E-13	NM_111463	rare cold inducible protein
CN635596.1	*Arabidopsis thaliana*	3.00E-42	NM_125822	phosphate-responsive protein
CN635661.1[a]	*Arabidopsis thaliana*	na	NM_117347	auxilin-related protein
CN635674.1	*Arabidopsis thaliana*	4.00E-47	NM_121534	pentatricopeptide (PPR) containing protein
CN635691.1	*Picea abies*	5.00E-112	AF328842	homeodomain protein (HB2)
CN636014.1	*Arabidopsis thaliana*	2.00E-112	NM_112093	heat shock protein 70 kDa
CN636043.1	*Pseudotsuga menziesii*	1.00E-95	U41902	cysteine protease pseudotzain
CN636093.1	*Cryptomeria japonica*	2.00E-19	AB211741	calmodulin
CN636149.1	*Pinus taeda*	6.00E-30	Z37992	cinnamyl alcohol dehydrogenase
CN636303.1	*Pinus radiata*	2.00E-91	EU301694	actin depolymerizing factor
CN636471.1	*Pinus pinaster*	8.00E-100	AY321089	phenylalanine ammonia-lyase
CN636492.1	*Oryza sativa*	2.00E-55	NM_001050492	phosphoethanolamine methyltransferase
CN636784.1	*Pinus contorta*	1.00E-127	AF187821	S-adenosylmethionine synthetase
CN636795.1	*Arabidopsis thaliana*	1.00E-59	NM_101028	xyloglucan:xyloglucosyl transferase
CN636901.1	*Oryza sativa*	8.00E-27	NM_001065251	alanine aminotransferase
CN636999.1[a]	*Arabidopsis thaliana*	na	NM_103822	BURP domain-containing protein
CN637166.1	*Arabidopsis thaliana*	2.00E-26	NM_100889	phloem protein
CN637226.1	*Arabidopsis thaliana*	7.00E-75	NM_100698	prephenate dehydratase family protein
CN637244.1	*Zea mays*	1.00E-28	NM_001112543	cysteine protease inhibitor
CN637306.1	*Picea glauca*	3.00E-61	EF601068	MYB-like transcription factor
CN637339.1	*Arabidopsis thaliana*	3.00E-45	NM_129573	unknown hypothetical protein
CN637910.1	*Arabidopsis thaliana*	3.00E-38	NM_101012	ABC family protein

CN637944.1	*Arabidopsis thaliana*	2.00E-32	NM_129387	bet v I domain containing protein
CN638015.1	*Picea sitchensis*	6.00E-15	EF084692	unknown hypothetical protein
CN638070.1	*Arabidopsis thaliana*	2.00E-24	NM_119071	acid phosphatase class B family protein
CN638367.1	*Oryza sativa*	1.00E-90	NM_001051693	ATP-dependent RNA helicase-like protein
CN638381.1	*Oryza sativa*	3.00E-117	NM_001069063	iron-inhibited ABC transporter
CN638489.1	*Oryza sativa*	2.00E-114	AF247164	alpha-expansin
CN638545.1	*Pinus taeda*	7.00E-90	AF096998	trans-cinnamate 4-hydroxylase
CN638556.1	*Arabidopsis thaliana*	1.00E-25	NM_120637	transcription regulation protein
CN638735.1	*Pinus taeda*	1.00E-123	DQ641986	cellulose synthase-like A1
CN639074.1	*Pinus contorta*	1.00E-34	U38186	S-adenosylmethionine synthetase
CN639087.1	*Arabidopsis thaliana*	7.00E-68	NM_124213	LRR receptor-like protein kinase
CN639130.1	*Arabidopsis thaliana*	4.00E-55	NM_118561	chloroplast heat shock protein 70 kDa
CN639236.1	*Oryza sativa*	3.00E-96	NM_001050445	guanine nucleotide-binding beta subunit protein
CN639311.1	*Oryza sativa*	2.00E-66	AB111916	replication protein
CN639346.1	*Pinus radiata*	5.00E-32	U90346	MADS-box transcription factor
CN639480.1	*Arabidopsis thaliana*	9.00E-41	NM_100032	2-hydroxyacid dehydrongenase
CN640037.1	*Pinus tabuliformis*	9.00E-79	DQ062681	tau class glutathione S-transferase
CN640110.1	*Arabidopsis thaliana*	4.00E-66	NM_110969	galacturonosyltransferase
CN640155.1	*Oryza sativa*	6.00E-38	NM_001068919	bicoid-interacting 3 domain containing protein
CN640247.1	*Picea mariana*	6.00E-87	AF227627	chalcone synthase
CN640289.1	*Oryza sativa*	9.00E-50	NM_001074378	serine hydroxymethyltransferase
CN640361.1	*Arabidopsis thaliana*	9.00E-92	NM_100263	zinc-finger (C2H2 type) family protein
CN640419.1	*Glycine max*	3.00E-96	AB210900	heat shock protein 70 kDa
CN640485.1	*Oryza sativa*	1.00E-69	NM_001070907	HNH endonuclease domain containing protein
CN640493.1	*Arabidopsis thaliana*	1.00E-39	NM_180904	nuclear transport factor
CN640521.1	*Arabidopsis thaliana*	6.00E-40	NM_179270	DNA-binding bromodomain-containing protein
CN640670.1	*Oryza sativa*	6.00E-55	NM_001062995	GH3 auxin-responsive promotor family protein
CN640738.1	*Ginkgo biloba*	1.00E-27	AY750963	anthocyanidin reductase
CN641116.1	*Oryza sativa*	3.00E-59	NM_001065234	carboxy-terminal kinesin
CN641171.1	*Arabidopsis thaliana*	4.00E-34	NM_106730	cinnamoyl CoA reductase

CN641226.1	*Glycine max*	1.00E-31	AB092811	LRR receptor-like protein kinase
ES418315.1	*Pinus pinaster*	3.00E-47	AJ309081	flavenoid 3-hydroxylase
ES418915.1	*Pinus radiata*	4.00E-24	AY262820	cellulose synthase-like protein
ES419198.1	*Pinus taeda*	7.00E-52	AY670436	LIM domain protein
ES419223.1[a]	*Arabidopsis thaliana*	na	NM_125984	phytosulfokine precursor
ES419242.1	*Oryza sativa*	1.00E-10	NM_001060766	response regulator protein
ES419657.1	*Arabidopsis thaliana*	1.00E-48	NM_114249	calmodulin
ES420171.1	*Arabidopsis thaliana*	1.00E-62	NM_114943	cold regulated plasma membrane protein
ES420250.1	*Picea abies*	6.00E-24	EF522166	dehydrin-like protein
ES420603.1	*Picea abies*	7.00E-21	EF522171	dehydrin-like protein
ES420757.1	*Arabidopsis thaliana*	6.00E-22	NM_123503	unknown hypothetical protein
ES420771.1	*Arabidopsis thaliana*	1.00E-30	NM_111461	anaphase promoting complex/cyclsome protein
ES420862.1	*Picea glauca*	3.00E-56	L42465	late embryo abundance (LEA) protein
ES421219.1	*Oryza sativa*	1.00E-46	NM_001065800	UDP-glucosyltransferase family protein
ES421311.1	*Picea sitchensis*	1.00E-52	EF084165	unknown hypothetical protein
ES421603.1	*Arabidopsis thaliana*	7.00E-64	NM_124985	heat shock protein 90 kDa
ES421877.1	*Arabidopsis thaliana*	4.00E-56	NM_128767	ccr4-NOT transcription complex protein
ES422367.1	*Pinus radiata*	2.00E-21	EU394120	ferritin
ES424016.1	*Glycine max*	6.00E-35	AF243377	glutathione S-transferase
ES428620.1	*Picea glauca*	3.00E-60	AF121198	14-3-3 protein
Pm_CL135Contig1	*Arabidopsis thaliana*	2.00E-152	NM_114400	cysteine proteinase
Pm_CL1400Contig1	*Oryza sativa*	2.00E-32	NM_001060573	alpha-L-arabinofuranosidase/beta-D-xylosidase
Pm_CL150Contig1	*Arabidopsis thaliana*	9.00E-24	NM_202741	phloem protein
Pm_CL1692Contig1	*Oryza sativa*	5.00E-23	NM_001064601	zinc-finger containing protein
Pm_CL1811Contig1	*Arabidopsis arenosa*	7.00E-74	AY333120	Swi2/Snf2-related chromatin remodeling ATPase
Pm_CL1814Contig1	*Arabidopsis thaliana*	2.00E-51	NM_124040	tetraspanin
Pm_CL1868Contig1	*Arabidopsis thaliana*	1.00E-61	NM_128676	actin depolymerizing factor
Pm_CL1982Contig1	*Oryza sativa*	8.00E-94	NM_001057633	peptide transporter
Pm_CL1994Contig1	*Picea abies*	5.00E-154	AJ868575	caffeate O-methyltransferase
Pm_CL1997Contig1	*Pinus taeda*	6.00E-50	EF619967	sucrose synthase

Pm_CL1Contig2	*Picea glauca*	2.00E-89	AF109917	glycine-rich RNA-binding protein
Pm_CL2089Contig1	*Arabidopsis thaliana*	4.00E-52	NM_119920	putative formide amidohydrolase
Pm_CL2133Contig1	*Arabidopsis thaliana*	6.00E-41	NM_179926	mitochondrial transcription termination factor
Pm_CL214Contig1	*Zea mays*	1.00E-62	NM_001111956	beta-tubulin
Pm_CL2282Contig1	*Arabidopsis thaliana*	5.00E-22	NM_114895	unknown hypothetical protein
Pm_CL234Contig1	*Arabidopsis thaliana*	8.00E-110	NM_104107	RAB GTPase
Pm_CL618Contig1	*Arabidopsis thaliana*	3.00E-66	NM_120688	tropinone reductase
Pm_CL61Contig1	*Picea abies*	3.00E-106	AJ271126	cyclosporin A-binding protein
Pm_CL73Contig1	*Arabidopsis thaliana*	5.00E-94	NM_124900	glycosyl hydrolase family protein
Pm_CL783Contig1	*Arabidopsis thaliana*	7.00E-34	NM_129353	SOUL heme-binding family protein
Pm_CL795Contig1	*Arabidopsis thaliana*	2.00E-47	NM_202438	WD-40 repeat family protein
Pm_CL855Contig1	*Vitis vinifera*	2.00E-85	DQ786632	flavonoid 3-hydroxylase
Pm_CL908Contig1	*Arabidopsis thaliana*	1.00E-32	NM_121323	GRAM-containing/ABA-responsive protein
Pm_CL919Contig1	*Arabidopsis thaliana*	1.00E-44	NM_106112	HVA22-like protein
Pm_CL922Contig1	*Arabidopsis thaliana*	5.00E-49	NM_001035987	thaumatin-like protein
Pm_CL939Contig1	*Arabidopsis thaliana*	1.00E-85	AY045869	aluminum-induced protein
Pm_CL969Contig1	*Oryza sativa*	6.00E-57	NM_001055522	cell division cycle protein
Pm_CL988Contig1	*Arabidopsis thaliana*	5.00E-14	NM_101026	thioredoxin-like protein
sM13Df243	*Pinus taeda*	5.00E-14	AY648093	arabinogalactan 4
sSPcDFD005F06506	*Arabidopsis thaliana*	3.00E-27	NM_115415	regulator of chromosome condensation protein
sSPcDFD015C12212	*Arabidopsis thaliana*	4.00E-49	NM_112443	phospholipase D
sSPcDFD024D11311	*Arabidopsis thaliana*	8.00E-53	NM_102304	polcalcin
sSPcDFD040B03103	*Pinus radiata*	4.00E-34	U42400	MADS-box transcription factor
sSPcDFE002A03003	*Picea glauca*	1.00E-33	L42466	ACC oxidase
sSPcDFE025C06206	*Oryza sativa*	9.00E-48	NM_001059265	purple acid phosphatase
sSPcDFE028B10110	*Arabidopsis thaliana*	6.00E-28	NM_117813	beta-amylase
sSPcDFE038D06306	*Arabidopsis thaliana*	8.00E-32	NM_130225	calcium binding protein with EF-hand motif
sSPcDFE044F10510	*Arabidopsis thaliana*	4.00E-35	NM_127816	mitochondrial substrate carrier family protein
sSPcDFE049B06106	*Arabidopsis thaliana*	2.00E-23	NM_130234	auxin-responsive family protein
sSPcDFE049E11411	*Arabidopsis thaliana*	3.00E-42	NM_202131	pentatricopeptide (PPR) containing protein

sSPcDFF014F08508	*Oryza sativa*	3.00E-34	NM_001056474	hypothetical water stress induced protein
sSPcDFF015H05705	*Oryza sativa*	1.00E-34	NM_001055452	cytochrome P450 family protein
sSPcDFF044H10710	*Arabidopsis thaliana*	6.00E-31	NM_125091	auxin:hydrogen symporter/transporter
U22458.1	*Populus tremula*	3.00E-159	AM_072292	phytochrome B
Z49715.1[a]	*Arabidopsis thaliana*	na	NM_104147	late embryogenesis abundant (LEA) protein

Annotations were based on tBLASTx analysis using the non-redundant nucleotide (nr/nt) collection available from GenBank. All analyses were conducted using the Douglas-fir expressed sequence tag (EST) or EST contig from which resequencing primers were designed as the query sequence. Hits against organisms without fully sequenced genomes were verified for similar gene functionality against the *Arabidopsis thaliana* and *Oryza sativa* genomes whenever possible. Douglas-fir candidate genes with similar gene products were designated as separate members of a gene family when nucleotide sequence similarity for overlapping EST or EST contigs was < 90%.

[a]These candidate genes had an extreme expression differences in Douglas-fir cold-hardiness EST libraries and were chosen based on this and results from blastp searches.

TABLE S3

Data summary and annotation information for 121 candidate genes; SD = standard deviation, UTR = untranslated region

Locus	Length [a] (bp)	Missing [b] (bp)	*n*	SDR[c]	BDR[d]	Frame [e]	5' UTR [f]	Exon [f]	Intron [f]	3' UTR [f]
CD028057.1	686	0	20	0	20	3		1-38, 177-292, 370-537, 668-686	39-176, 293-369, 538-667	
CN634517.1	777	2	23	0/0	23/23	1		1-71, 191-686	72-190	687-777
CN634677.1	288	0	23	3	20	3		1-288		
CN635137.1	738	3	21	0	21	2		1-231	232-738	
CN635490.1	448	27	23	1	22	1		1-99, 222-311	100-221	312-448
CN635596.1	311	0	23	7	16	2		1-212		213-311
CN635661.1	254	12	20	0	20	3		1-166		167-254
CN635674.1	163	0	19	9	10	2		1-163		
CN635691.1	635	16	23	0	23	2		1-56, 181-355, 510-635	57-180, 356-509	
CN636014.1	675	0	24	0/0	24/24	2		1-675		
CN636043.1	1176	32	22	0	22	2		1-83, 959-1033	84-958	1034-1176
CN636093.1	353	0	22	0	22	2		1-80		81-353
CN636149.1	341	0	18	0	18	1		1-89, 187-341	90-186	
CN636303.1	650	0	23	0	23	1		1-104, 239-389	105-238	390-650
CN636471.1	433	1	23	0	23	2		1-433		
CN636492.1	406	0	24	0	24	3		1-29, 207-406	30-206	
CN636784.1	803	0	24	0/0	24/24	3		1-803		
CN636795.1	676	14	23	0	23	1		200-396, 520-676	1-199, 397-519	
CN636901.1	569	0	23	0	23	1		1-14, 143-269	15-142	270-569
CN636999.1	357	0	23	0	23	2		1-53, 164-357	54-163	
CN637166.1	366	48	16	0	16	3		1-366		
CN637226.1	188	23	20	0	20	3		1-188		

CN637244.1	366	2	22	0	22	3		1-169, 263-366	170-262
CN637306.1	670	5	23	1	22	2		1-90, 196-325, 627-670	91-195, 326-626
CN637339.1	533	0	22	0	22	1		1-32, 109-280, 377-533	33-108, 281-376
CN637910.1	303	0	23	0	23	1		1-303	
CN637944.1	237	0	20	5	15	2		1-237	
CN638015.1	395	2	21	0	21	2		1-139, 229-268	140-228	269-395
CN638070.1	185	0	12	0	12	3		1-185	
CN638367.1	889	4	23	0	23	2		1-101, 483-575, 696-781, 864-889	102-482, 576-695, 782-863
CN638381.1	959	0	16	0	16	3		1-853		854-959
CN638489.1	456	30	15	3	12	3		1-147, 253-456	148-252
CN638545.1	512	0	23	0	23	2		1-386		387-512
CN638556.1	380	0	23	0	23	3		1-380	
CN638735.1	596	0	23	0	23	2		1-79, 251-442, 589-596	80-250, 443-588
CN639074.1	547	0	24	0	24	3		1-238		239-547
CN639087.1	370	0	23	3	20	1		1-370	
CN639130.1	117	0	21	0	21	3		1-117	
CN639236.1	308	0	20	0	20	2		1-308	
CN639311.1	812	22	22	0	22	3		1-43, 144-304	44-143, 305-812
CN639346.1	189	2	17	2	15	1	1-57	58-189	
CN639480.1	422	0	23	0	23	3		1-422	
CN640037.1	458	0	22	0	22	2		1-188, 300-458	189-299
CN640110.1	364	0	23	0	23	2		1-364	
CN640155.1	318	36	17	1	16	3		1-318	
CN640247.1g	754	1	24	0	24	2		1-602 (605)		603 (606)-754
CN640289.1	228	0	23	0	23	3		1-208		209-228
CN640361.1	757	7	22	6	16	1		1-82, 687-757	83-686
CN640419.1	618	1	22	0	22	2		1-15, 114-268, 358-440, 548-618	16-113, 269-357, 441-547

ID	Length							Col1	Col2	Col3
CN640485.1	528	2	23	0	23	1	1-72	73-298, 502-528	299-501	
CN640493.1	247	0	16	0	16	3		1-94, 215-247	95-214	
CN640521.1	418	0	23	0	23	1		1-418		
CN640670.1	197	0	23	1	22	2		1-197		
CN640738.1	542	0	21	0	21	2		1-88, 199-340	89-198	341-542
CN641116.1	739	40	23	0	23	1		1-77, 322-403, 525-629, 735-739	78-321, 404-524, 630-734	
CN641171.1	470	0	22	0	22	2		1-157, 244-445	158-243	446-470
CN641226.1	375	0	23	0	23	2		1-375		
ES418315.1	426	1	22	0	22	1		1-426		
ES418915.1	401	0	23	0	23	3		1-100		101-401
ES419198.1	368	1	23	0	23	1		1-147		148-368
ES419223.1	445	5	22	0	22	3		1-34, 134-292	35-133	293-445
ES419242.1	831	0	16	0	16	1		1-11, 529-727	12-528	728-831
ES419657.1	377	0	23	0	23	3		1-178		179-377
ES420171.1	235	0	23	0	23	1		1-90		91-235
ES420250.1	884	13	23	0	23	1	1-124	125-241, 368-655	242-367	656-884
ES420603.1	425	0	23	0	23	3		1-295		296-425
ES420757.1	648	0	19	0	19	2		1-23, 174-329, 474-648	24-173, 330-473	
ES420771.1	292	0	20	0	20	3		1-127		128-292
ES420862.1	679	49	23	0	23	3		1-10, 143-583	11-142	584-679
ES421219.1	499	0	22	0	22	2		1-494		495-499
ES421311.1	729	0	21	0	21	1		1-113, 397-532	114-396	533-729
ES421603.1	528	0	23	0	23	1		1-411		412-528
ES421877.1	550	0	19	0	19	2		1-488		489-550
ES422367.1	1038	24	16	0	16	2		273-334, 453-518, 625-688, 850-929	1-272, 335-452, 519-624,689-849	930-1038
ES424016.1	397	0	21	0	21	1		1-345		346-397
ES428620.1	686	0	17	0	17	1		206-322, 433-492	1-205, 323-432	493-686
Pm_CL135Contig1	769	1	8	6	2	1		1-132, 256-387, 761-769	133-255, 388-760	

Pm_CL1400Contig1	378	1	23	2	21	3		1-325		326-378
Pm_CL150Contig1	356	40	16	0	16	2		1-356		
Pm_CL1692Contig1	358	4	22	1	21	1	1-16	17-358		
Pm_CL1811Contig1	672	32	16	0	16	1		204-323, 527-625	1-203, 324-526, 626-672	
Pm_CL1814Contig1	368	0	23	0	23	1		1-368		
Pm_CL1868Contig1	398	1	21	0	21	3		1-151		152-398
Pm_CL1982Contig1	271	0	23	0	23	1		1-271		
Pm_CL1994Contig1	831	0	23	0/0	23/23	2		1-210, 299-363, 484-783	211-298, 364-483	784-831
Pm_CL1997Contig1	711	12	21	0	21	2		227-339, 462-581	1-226, 340-461	582-711
Pm_CL1Contig2	631	19	16	0	16	1	1-103	104-217, 532-631	218-531	
Pm_CL2089Contig1	400	0	23	0	23	1	1-123, 222-234	235-400	124-221	
Pm_CL2133Contig1	334	0	23	1	22	3		1-334		
Pm_CL214Contig1	360	0	22	9	13	3		1-259		260-360
Pm_CL2282Contig1	351	3	23	0	23	1		1-351		
Pm_CL234Contig1	753	5	18	0	18	1		74-223, 334-414, 733-753	1-73, 224-333, 415-732	
Pm_CL618Contig1	348	44	23	3	20	2		1-126, 297-348	127-296	
Pm_CL61Contig1	392	28	21	1	20	2		1-116		117-392
Pm_CL73Contig1	462	31	23	0	23	1		1-151, 265-299	152-264	300-462
Pm_CL783Contig1	406	0	22	2	20	2		1-380		381-406
Pm_CL795Contig1	417	7	23	0	23	3		1-316		317-417
Pm_CL855Contig1	394	0	23	0	23	3		1-358		359-394
Pm_CL908Contig1	501	5	18	0	18	2		1-101, 204-449	102-203	450-501
Pm_CL919Contig1	738	10	22	1	21	2		1-13, 110-344, 693-738	14-109, 345-692	
Pm_CL922Contig1	433	0	22	1	21	3		1-349		350-433
Pm_CL939Contig1	437	0	21	0	21	2		1-133, 218-437	134-217	
Pm_CL969Contig1	404	0	23	1	22	3		1-247		248-404
Pm_CL988Contig1	555	8	23	0	23	1		1-45, 241-555	46-240	

sM13Df243	286	0	19	0	19	1		1-231		232-286
sSPcDFD005F06506	507	56	21	0	21	2		1-35, 161-280	36-160	281-507
sSPcDFD015C12212	152	0	23	10	13	3		1-28		29-152
sSPcDFD024D11311	388	16	23	1	22	1		1-388		
sSPcDFD040B03103	378	0	22	0	22	3		1-210		211-378
sSPcDFE002A03003	501	0	12	1	11	2		1-140, 223-465	141-222	466-501
sSPcDFE025C06206	456	9	13	3	10	2		1-197, 410-456	198-409	
sSPcDFE028B10110	431	0	22	0	22	2		1-407		408-431
sSPcDFE038D06306	386	44	23	0	23	1	1-38	39-386		
sSPcDFE044F10510	353	33	23	0	23	1		1-353		
sSPcDFE049B06106	358	3	21	0	21	2		1-293		294-358
sSPcDFE049E11411	407	0	20	0	20	3		1-325		326-407
sSPcDFF014F08508	499	0	13	0	13	2		1-53, 168-404	54-167	405-499
sSPcDFF015H05705	286	0	23	11	12	3		1-271		272-286
sSPcDFF044H10710	674	0	16	0	16	3		1-61, 260-336, 425-491	62-259, 337-424, 512-588	492-511, 589-674
U22458.1	706	0	23	0	23	3		1-706		
Z49715.1	984	91	20	0/0	20/20	2		1-5, 410-697, 821-934	6-409, 698-820	935-984
Total	59173	928	----							
Average (±1 SD)	489 (±204)	8 (±15)	21 (±3)							

^{a}The length in base pairs of the aligned data.

^{b}The number of aligned positions where at least one sample has missing data or an insertion-deletion (indel) event.

^{c}SDR = single direction read. The number of samples with single, either forward or reverse, reads. Loci with two primer sets give results for each set separated by a slash.

^{d}BDR = bidirectional reads. The number of samples with both forward and reverse reads. Loci with two primer sets give results for each set separated by a slash.

^{e}Frame is given as the codon position of the first base in the alignment or the first base within the coding region.

^{f}Ranges are given as positions in the alignment with the numbering starting at 1.

^{g}This locus had a point mutation in some samples that extended the coding region for an extra amino acid. Values for this haplotype are given in parentheses.

TABLE S4

A list of primers by locus for all 121 candidate genes resequenced within the diversity panel of coastal Douglas-fir

Locus	Forward primer (5'-3')	Reverse primer (5'-3')	AT (°C)	Primer sets
CD028057.1	AACGTCTTACGGCTGCTGAG	GGCTTGACCAATACCACAGAA	57	1
CN634517.1	AATCAGGAGTGCCAAGACCG	GCCTCTCTTTGATTTTATTCTCCCA	55	2
	GGACAAGCACCAGAGCACGA	CGAGGGAAGTCCAAATCTGAAGTA	55	
CN634677.1	AACACGCTCTCGTATTGCC	GCTTTTCCAGTCAGAATC	60	1
CN635137.1	CAAGGGAATGAACTGAAGTTGGTG	CAAATGGCTCCCAAACACTGA	55	1
CN635490.1	TCAACACATACCCATAGTCGCAC	GGTTGGGTGTGTAAATATGTC	55	1
CN635596.1	GTTTTTTTCAGGGCGACGG	AGTAAAAGGATTTGTAACAGCCACCAG	60	1
CN635661.1	AAGAAGGGCAGAAAGAGCAGCAC	TGCTCTCTCTGCCCGTTCCCTTG	55	1
CN635674.1	CTTCATAGGCGTTTTGTC	GCTTCAGGTTTTACTGG	60	1
CN635691.1	GAGAAAATTCGCCTTCAG	CATCGTCATCAATGTTACC	60	1
CN636014.1	TTGTCTCTTGGATTGGAAACTGC	TTCATCCTCAGCGTTGTATTTCTCT	55	2
	TGAAGGTGAAAGAGCAAGGA	ACCAGAAGCTCCACCAAAAG	55	
CN636043.1	TATGACTTTGGGGGTTACTGCTATG	ATTGACGAGAACACTGAGGGGAA	55	1
CN636093.1	GAGCCAGCACAGCGAAACAT	ACTATGATGTGGAAAGCAAAACC	55	1
CN636149.1	TCCAAACAACCTTCTCGCAGTATT	ACGACGTAACATTCAAGGTAGCA	55	1
CN636303.1	CCCCCATCCCAAAAGTTAAT	CAAACTTATGGCGACTTCAC	55	1
CN636471.1	GCGTGGTCTCTCAGGTGGC	CCTTTCCGATGTATTCACCCG	55	1
CN636492.1	GGAGAAGGATTTGTCAGTACGGGA	CTCAAATTCAACAGCACATCGTC	55	1
CN636784.1	GGTTGAGACCAGATGGGAAA	TTTCCTTGTCTGGGATCCTG	55	2
	TCCCTGAGGTGCTGTTCTCT	AGGGCTCTGCTGTTCAATGT	55	
CN636795.1	ACAGATTCGGGTGGTTCAGCAT	ACGAAGATACAAATGGAGCAGC	55	1
CN636901.1	CCTGGTTCAGGATTCGGTCAA	GCGTGTGTTTATGATTTTTATGATGTG	55	1
CN636999.1	AGGATTTGCTTTCACTGGAGAGA	CATTCACTCCTCCCTTGCCA	55	1
CN637166.1	CCAGAAGATGAAGAATCC	TGAAGCCCTGTAAAACTCC	60	1

CN637226.1	AATCGGGTCATTAGCC	CGTTGTTACAGTCGTC	60	1
CN637244.1	AAATGCCGACGAGATGCTGC	GCCGCATACAGCTTGGTTTTA	55	1
CN637306.1	CTAAACAATGGGAAGGG	ATCTCGTTGTCCGTTC	60	1
CN637339.1	AGGATGGAGATGGCAAC	CTGAACTGAAGACGAG	60	1
CN637910.1	GCACCGTCACATAAATTTTC	TTCATCAAGTCGCAGCC	60	1
CN637944.1	ATGTCTGGTCCGTGTTG	TCCCATCTTTCTCCTC	60	1
CN638015.1	TCCAATCTACTCAAGGCGTCCA	CAGTCTTAGCAGCGAAATAACAACA	55	1
CN638070.1	GTTTCTCTTGTTCCTCCTC	GCATCATATACTTCTTCACATAGCC	60	1
CN638367.1	CTTCCTGAGCAAACCCTGAGC	GCATAAAGTGTCGGAAGGAAAGGAT	55	1
CN638381.1	TTGAGGAAAACCAGATGAAGCAGT	CTGCTACCAAAGTCAAACATAATCAATACA	57	1
CN638489.1	ACCAATTTCTGCCCTCC	GATAAAGTCTGCCCAACC	60	1
CN638545.1	TTCCGCTCCTCGTTCCTCACAT	GCAAAACTACTGACAGCAAAAACAA	55	1
CN638556.1	ATGGGGTGAGCGTTATCTGG	CAACTCTCAGTCATATCAGG	60	1
CN638735.1	CCTTTTACTGTGTTGTGATTCC	GAAGAAGAGATAGACACC	60	1
CN639074.1	AGTGCCCGAACCTCTGTCTGT	AAGCCATTACATCCAAAGCGT	57	1
CN639087.1	AGACAGAAAAGCAGTTCAAG	ATAACCCAAGTCACCAAAATCACC	60	1
CN639130.1	CTCATTGAGAGATGCAAAG	GGATTCACAGTAACATTTGG	60	1
CN639236.1	TTCTCCATTGATAACCGCCAG	ATAGTAACTCCGTCTTTGCCGCCGT	55	1
CN639311.1	CTATGGCATCTGTTGG	GCTGAAGGATTTGCTC	60	1
CN639346.1	CAACTGAGCAACTCCGACTGATT	CCACTTCGGCATCGCAGAGC	55	1
CN639480.1	ATCATTCGCATGAGGG	GGGTTTCTTCATCATAACAG	60	1
CN640037.1	CTGCTGCAATCAAACC	TCAACCAAACCAATCCC	60	1
CN640110.1	ATTGTCTCACTCTGCGG	CGAATTTCAATATGCGTCTC	60	1
CN640155.1	GAAGATAAGGGCAGAG	CGAATCAACCATTCATCAC	60	1
CN640247.1	TATTTACGCTTTCTCCCGAT	AATTCTTCCCGACAGCGACG	55	1
CN640289.1	AGCCGATTTTGAGAAGATTGGAGAG	TATGCTATTCCTATGGTCACTTATCGG	55	1
CN640361.1	AATCCAATGTTACTTCTGCTGCTTC	ATCTCCTTGCTAGTCCGCTGTCTC	60	1
CN640419.1	TGGAGAAGGTGGAGAAGAAA	TTCCAGTGCCATTGTCCTCT	55	1
CN640485.1	CACATTTATCCCCTCTC	TTGGCAATTCTCAACTGTAGTC	60	1
CN640493.1	ATGTTCTCCACCAGTCTCCCCAAATG	GGTTGTAAGAATCCTGAGAGTCCA	55	1

CN640521.1	AGCGGATGTCAGATTG	GGGTAGACTTTGTAGG	60	1
CN640670.1	ATATTGGGAATTGGTACGG	TTCTGGTGAGGATGTGG	60	1
CN640738.1	ACATCCAGGTTGCCATTGCG	CGCAGAAGGCCGCTACATTT	55	1
CN641116.1	TTCTCGCACCTTTTCCC	GCCATAATGACATCCCC	60	1
CN641171.1	AACTCAGGTATATGTGGATGTAAGGG	CCGAGGAACAGTGGAGAGAG	55	1
CN641226.1	GTGAGATCACCAATATTCAG	CTCCAAACATTGAAGGAATC	60	1
ES418315.1	GCAGCGGTGGTGAAAGAGACT	CAGATGGGAAGGAAGACGAGCA	55	1
ES418915.1	AGCCATTGCCTACTATTCTGTG	CTTCTTGCATCCATATTCTCCCTG	55	1
ES419198.1	TGGTGTTGTGTCATCAGTCCCTCA	GTCATACACAAGCCATAGCGATTAC	55	1
ES419223.1	CCCAAGTTCAAGTTTATTTCATCATC	AAATGAAGGATACAAACAAACTGCTC	55	1
ES419242.1	ATTGCATGCCCAGGAACTACAG	AGTCTTCGGCTCCTTCATCTAAA	57	1
ES419657.1	AAGCATTCCGGGTTTTCGAC	TATCACCCAGGACATTCAAAAAGTTAT	55	1
ES420171.1	CAAGAGCACATCCGACGCAA	ATTCCTCGGTCCATCCTTCTCT	55	1
ES420250.1	GTGGTGTCAGGTGGAAGGACAGT	CATCAAAGAGAAAATACAGTCGGC	55	1
ES420603.1	GAAGGAAGAAGAGGAAGGCGAGA	TCCGACGCATCTTACACATTATTA	55	1
ES420757.1	CCAATGCGGCGTGTGTTCAGTA	TTTTACAAGTTCAGCAAGACCACA	55	1
ES420771.1	CATTGGTATGGGGTGCGTGTA	TTCCAAGCAATGGCTGTTCAC	55	1
ES420862.1	AAAGACAGAGGTGAAAGAGATTGC	AACATCTCAAAGTATTCATCATCTCAA	55	1
ES421219.1	GGCGTTGGGAGAGGATTTTTC	AATCTTCCTCTTCTAATGCCACCA	55	1
ES421311.1	ATCCTTAGTCCGACATTTTGCTGCT	AAGGCACTACACAATACAAACGACAC	55	1
ES421603.1	CGACCTCCTCCATCTTGCTG	CGACCGTGTTGTGGATTCTC	55	2
	TCAAGCAAGAAGACAATGGAAATAAAT	GTCCACATAAATCCAAAATAAAACAGT	57	
ES421877.1	ATTCCATCGAGTTGCTACGCCAG	CCAACATAATAGGTCTCCATCAACG	55	1
ES422367.1	GACAATGCTGAGAAGGGCGA	ATACAAATCGCGGCTACCAAAAT	55	1
ES424016.1	TGTCAACCAGCGGGGATACTCA	TCTTTTGTTTCGTCACCTCCC	55	1
ES428620.1	ATAGACTCCACCAATCCGCT	TTGAATTCGCCAGATAGAGC	55	1
Pm_CL135Contig1	CTCACTAACACCATACC	GAGCATTTAACAACTTTGGG	60	1
Pm_CL1400Contig1	TGCGTCACTCTAATGCC	ATCTGTCAAAGTAGAGAACACC	60	1
Pm_CL150Contig1	CACTCTTTCTTTCAGGTTAC	CAAATCCTTCATTGTCTCCTTC	60	1
Pm_CL1692Contig1	CTTCAGGGTTAAAGAATGG	TGCGGAGAAGATGATG	60	1

Pm_CL1811Contig1	GTTTGTCGCATTGATGG	TGGAGCAACGCAAGTAG	60	1
Pm_CL1814Contig1	TAATGCCTCAGCCATCC	GCAGTAAGCAACAGTATTACAG	60	1
Pm_CL1868Contig1	GTCTCCTGACAAATCC	GTAGACCGTAGAATCC	60	1
Pm_CL1982Contig1	CTGAAAAAGTCGGAATTTGG	GCTAATAACATCAAATGCGG	60	1
Pm_CL1994Contig1	TGTGGGTGGAGATATG	CCAAGTGGAATATGGAATGAAG	60	2
	GAGATACAACAGTATTTTCAACAGGGG	AAGTGTCATGCAATAATTATCACCCC	60	
Pm_CL1997Contig1	GATTAATGACGCTGTCTG	CCCCTCCATACAAAATAC	60	1
Pm_CL1Contig2	CTGGTTCTCTTTGGTTC	TGCCATTCATTGCGTC	60	1
Pm_CL2089Contig1	GTTGTGAAAGACTTCCC	CACCCCCACTAAAATC	60	1
Pm_CL2133Contig1	GCCAACACTCTATTTTTTGC	CTCAACATCGTTTTCAACC	60	1
Pm_CL214Contig1	CCAACAATGTGAAATCCAG	GCCTACGAAACAACAAGAAATG	60	1
Pm_CL2282Contig1	AAATCCTGCCCTTGTC	AAATCTCTTCCTCCTCC	60	1
Pm_CL234Contig1	GAAGTGGAAGTGGAAGATAG	ACATTCATGTCCTCCTTAGCTG	60	1
Pm_CL618Contig1	CAGCTTATCATCTGTCTC	TTGTCACTTGCCCACTC	60	1
Pm_CL61Contig1	AACCTGCTGAAAACCC	TCTTCGGTCAAGTCGTC	60	1
Pm_CL73Contig1	GATTGCCAGCAGATTCAACC	AATAAGTAAGAATGATACAGCCAGCCC	60	1
Pm_CL783Contig1	AAAGCTCTCCAGAGTCCCAACC	GTCGAAAAAGAAAACACCATATTCCCC	60	1
Pm_CL795Contig1	GGACATTCATACACGG	TAGACTTTGGGATGTTAGG	60	1
Pm_CL855Contig1	ACATTCCCAAGAACGCC	CACTTCAAATGTCTGCC	60	1
Pm_CL908Contig1	CAAACTCTGGACAACAC	CGGAACTCTGTATATCTC	60	1
Pm_CL919Contig1	ATCAACAGTGGCTGAC	CAGTATATGATCCAAATGGG	60	1
Pm_CL922Contig1	CAACTACATTTTCGTCGG	GGATGGCTACAATCTTC	60	1
Pm_CL939Contig1	CAGACCAGAGGAAAAC	GGAAGTGGAGTCATAAAG	60	1
Pm_CL969Contig1	GGAGGATGATACTGAAG	CAGATTTCCATAGCATAGAC	60	1
Pm_CL988Contig1	TTATCAGGCTTCGGCTTCGG	TCTGAAGGTGGACTCTGAC	60	1
sM13Df243	AGTCCGTAAACGGGCTTTCT	CGTGGAAACCGAGGAAGTAG	55	1
sSPcDFD005F06506	GAAGGTACAGTATAGGAATG	AAGTCTTTGCTGGGG	60	1
sSPcDFD015C12212	CTCTAAAGACTTCTCTCTG	TTACCTGCCACCCATTC	60	1
sSPcDFD024D11311	CATCAATCTACAGTCCTCC	TCGAATCAAATCGAATCCAGCC	60	1
sSPcDFD040B03103	GCGGGAGAAAAATTAAAGG	GGAGAAGGAAAGAATGG	60	1

sSPcDFE002A03003	CATTAACCCAACAAACCAC	TCATACAGATGGAGGAG	60	1
sSPcDFE025C06206	CAACTCCAATGTGCTTC	CCAATACAAGTGGCTTC	60	1
sSPcDFE028B10110	GAGATTTGAGATGTGTTGAG	CTGCTTTGAGATGAAGG	60	1
sSPcDFE038D06306	TTACAGTTGGTTAGGGTTTC	AATTGGGGTTTCAATCAAGGCTTC	60	1
sSPcDFE044F10510	GTCCTTGAAAACCTTCC	CATGATCGTTGACAGCC	60	1
sSPcDFE049B06106	CAACCATAACAGCAACAC	GCCACGATTTTCACAAG	60	1
sSPcDFE049E11411	CAACACCTGCAAAACTC	GGCATCTATGTACTGGTTAATC	60	1
sSPcDFF014F08508	TGACGTGAAGGAACTG	CTGAGAATGTGGATTTGG	60	1
sSPcDFF015H05705	CAGCAGCATTAAAGATGG	GGATGGAGAGTGTTTGG	60	1
sSPcDFF044H10710	CTGTGTTTTAGGTCTCTC	TCGCAATGGCTGTTAG	60	1
U22458.1	CAATTTTGGTCCACTCCAAG	AATCCCAAAAACTTGCATCA	57	1
Z49715.1	AGGCAACTGAAACGACCAAGG	TAAAACCAGCCAAGCCAAACAA	57	2
	CGACGATGAAGAGGAGGGAG	TAATCAAAACCACACAACACGCAC	57	

Genomic DNA was amplified in 384-well format PCR setup. Each PCR reaction contained 10 ng DNA, 1x HotStart buffer (Qiagen, Valencia, CA), 0.8 mM dNTPs, 1 mM MgCl$_2$, 0.2 U HotStart polymerase (Qiagen) and 0.2 uM forward and reverse primers in 10 ul reactions. PCR cycling parameters were: one cycle of 95ºC for 15 min, 35 cycles of 95ºC for 20 s, 55-60ºC for 30 s and 72ºC for 1 min, followed by one cycle of 72ºC for 3 min. The resultant PCR products were purified using the AMPure® solid phase reversible immobilization chemistry (Agencourt Bioscience, Boston, MA) followed by bidirectional dideoxy sequencing with universal M13 primers and the Big-Dye v. 3.1 chemistry (Applied Biosystems, Foster City, CA). Sequencing was carried out via capillary electrophoresis using an ABI Prism 3730XL DNA analyzer. AT = annealing temperature.

A. J. Eckert *et al.*

TABLE S5

Common measures of nucleotide and haplotype diversity for 121 candidate genes

Locus	All					Sil			Syn			Nonsyn		
	S^a	$\theta_W{}^b$	$\theta_\pi{}^c$	h^d	$H_d{}^e$	S^a	$\theta_W{}^b$	$\theta_\pi{}^c$	S^a	$\theta_W{}^b$	$\theta_\pi{}^c$	S^a	$\theta_W{}^b$	$\theta_\pi{}^c$
CD028057.1	1	0.00041	0.00064	2	0.442	1	0.00068	0.00106	0	0.00000	0.00000	0	0.00000	0.00000
CN634517.1	5	0.00175	0.00084	7	0.598	5	0.00333	0.00172	3	0.00711	0.00415	1	0.00060	0.00019
CN634677.1	1	0.00094	0.00082	2	0.237	1	0.00365	0.00319	1	0.00365	0.00319	0	0.00000	0.00000
CN635137.1	25	0.00945	0.00904	15	0.943	24	0.01280	0.01163	3	0.01442	0.01872	1	0.00163	0.00291
CN635490.1	5	0.00322	0.00291	4	0.549	4	0.00384	0.00327	2	0.01139	0.00817	1	0.00196	0.00217
CN635596.1	13	0.01133	0.00844	6	0.672	10	0.01745	0.01425	6	0.03041	0.02900	3	0.00529	0.00273
CN635661.1	3	0.00349	0.00600	3	0.568	3	0.00677	0.01162	1	0.00832	0.01493	0	0.00000	0.00000
CN635674.1	6	0.01053	0.00861	4	0.614	1	0.00896	0.00330	1	0.00896	0.00330	5	0.01126	0.01022
CN635691.1	2	0.00088	0.00028	3	0.170	1	0.00081	0.00026	0	0.00000	0.00000	1	0.00105	0.00034
CN636014.1	7	0.00278	0.00296	5	0.670	7	0.01282	0.01374	7	0.01285	0.01371	0	0.00000	0.00000
CN636043.1	28	0.00671	0.00599	9	0.883	28	0.00724	0.00620	0	0.00000	0.00000	0	0.00000	0.00000
CN636093.1	1	0.00078	0.00104	2	0.368	1	0.00094	0.00127	0	0.00000	0.00000	0	0.00000	0.00000
CN636149.1	5	0.00426	0.00542	8	0.830	4	0.00786	0.01181	0	0.00000	0.00000	1	0.00151	0.00058
CN636303.1	1	0.00042	0.00013	2	0.087	1	0.00060	0.00019	0	0.00000	0.00000	0	0.00000	0.00000
CN636471.1	15	0.00941	0.01008	9	0.850	9	0.02403	0.02766	9	0.02403	0.02766	6	0.00496	0.00473
CN636492.1	1	0.00066	0.00039	2	0.159	1	0.00116	0.00069	0	0.00000	0.00000	0	0.00000	0.00000
CN636784.1	9	0.00300	0.00191	6	0.543	8	0.01095	0.00741	8	0.01095	0.00741	1	0.00044	0.00014
CN636795.1	16	0.00655	0.00705	8	0.850	13	0.00915	0.01074	4	0.01426	0.01373	3	0.00292	0.00191
CN636901.1	6	0.00286	0.00445	4	0.719	6	0.00355	0.00553	0	0.00000	0.00000	0	0.00000	0.00000
CN636999.1	0	0.00000	0.00000	1	0.000	0	0.00000	0.00000	0	0.00000	0.00000	0	0.00000	0.00000
CN637166.1	4	0.00379	0.00259	4	0.442	3	0.01174	0.00768	3	0.01174	0.00768	1	0.00127	0.00098
CN637226.1	6	0.01025	0.01515	7	0.879	3	0.02156	0.03275	3	0.02156	0.03275	3	0.00689	0.00990
CN637244.1	6	0.00452	0.00463	7	0.697	6	0.01050	0.01074	4	0.01669	0.01731	0	0.00000	0.00000
CN637306.1	18	0.00733	0.00617	9	0.850	17	0.00995	0.00867	3	0.01310	0.01006	1	0.00136	0.00044

CN637339.1	22	0.01132	0.01131	8	0.827	15	0.01638	0.01661	7	0.02423	0.02114	7	0.00684	0.00662
CN637910.1	5	0.00447	0.00451	7	0.830	5	0.01871	0.01889	5	0.01871	0.01889	0	0.00000	0.00000
CN637944.1	8	0.00951	0.00680	8	0.816	4	0.01900	0.01322	4	0.01900	0.01322	4	0.00645	0.00473
CN638015.1	13	0.00919	0.00737	7	0.810	12	0.01265	0.00903	2	0.01191	0.01102	1	0.00218	0.00404
CN638070.1	6	0.01074	0.00934	5	0.667	2	0.00909	0.01123	2	0.00909	0.01123	4	0.01081	0.00742
CN638367.1	9	0.00276	0.00141	6	0.518	8	0.00336	0.00157	1	0.00408	0.00250	1	0.00115	0.00100
CN638381.1	1	0.00031	0.00042	2	0.400	1	0.00100	0.00133	1	0.00158	0.00209	0	0.00000	0.00000
CN638489.1	9	0.00650	0.00608	6	0.762	9	0.01568	0.01468	5	0.02092	0.02255	0	0.00000	0.00000
CN638545.1	7	0.00370	0.00332	5	0.545	7	0.00882	0.00791	1	0.00315	0.00469	0	0.00000	0.00000
CN638556.1	2	0.00143	0.00243	3	0.664	2	0.00635	0.01083	2	0.00635	0.01083	0	0.00000	0.00000
CN638735.1	1	0.00045	0.00086	2	0.514	1	0.00071	0.00135	0	0.00000	0.00000	0	0.00000	0.00000
CN639074.1	4	0.00196	0.00131	5	0.612	3	0.00220	0.00174	0	0.00000	0.00000	1	0.00147	0.00046
CN639087.1	1	0.00073	0.00024	2	0.087	1	0.00319	0.00103	1	0.00319	0.00103	0	0.00000	0.00000
CN639130.1	2	0.00475	0.00798	2	0.467	0	0.00000	0.00000	0	0.00000	0.00000	2	0.00644	0.01081
CN639236.1	7	0.00641	0.00731	10	0.921	6	0.02250	0.02409	6	0.02250	0.02409	1	0.00122	0.00192
CN639311.1	3	0.00104	0.00035	4	0.260	2	0.00087	0.00029	0	0.00000	0.00000	1	0.00175	0.00058
CN639346.1	3	0.00475	0.00495	2	0.309	3	0.01022	0.01067	0	0.00000	0.00000	0	0.00000	0.00000
CN639480.1	9	0.00578	0.00616	8	0.798	6	0.01515	0.01399	6	0.01515	0.01399	3	0.00260	0.00351
CN640037.1	16	0.00958	0.00799	20	0.991	6	0.00867	0.00506	3	0.01044	0.00346	10	0.01031	0.01013
CN640110.1	2	0.00149	0.00091	2	0.166	1	0.00306	0.00188	1	0.00306	0.00188	1	0.00100	0.00061
CN640155.1	3	0.00315	0.00125	3	0.228	1	0.00515	0.00205	1	0.00515	0.00205	2	0.00267	0.00106
CN640247.1	8	0.00285	0.00211	5	0.529	8	0.00899	0.00698	3	0.00562	0.00606	0	0.00000	0.00000
CN640289.1	2	0.00238	0.00437	4	0.759	1	0.00426	0.00783	1	0.00667	0.01226	1	0.00166	0.00305
CN640361.1	21	0.00768	0.01045	12	0.926	21	0.00906	0.01205	2	0.01448	0.01736	0	0.00000	0.00000
CN640419.1	4	0.00178	0.00272	3	0.584	4	0.00296	0.00452	0	0.00000	0.00000	0	0.00000	0.00000
CN640485.1	8	0.00412	0.00340	8	0.854	5	0.00416	0.00403	2	0.01044	0.00625	3	0.00677	0.00359
CN640493.1	3	0.00366	0.00307	4	0.525	1	0.00205	0.00085	0	0.00000	0.00000	2	0.00608	0.00639
CN640521.1	6	0.00389	0.00475	4	0.636	4	0.01230	0.01122	4	0.01230	0.01122	2	0.00165	0.00303
CN640670.1	0	0.00000	0.00000	1	0.000	0	0.00000	0.00000	0	0.00000	0.00000	0	0.00000	0.00000
CN640738.1	22	0.01128	0.01281	10	0.900	17	0.01289	0.01455	2	0.01080	0.01517	5	0.00801	0.00928

CN641116.1	21	0.00813	0.00756	8	0.787	21	0.01147	0.01066	3	0.01214	0.00508	0	0.00000	0.00000
CN641171.1	6	0.00350	0.00297	4	0.619	5	0.00691	0.00473	2	0.00649	0.00409	1	0.00102	0.00169
CN641226.1	3	0.00217	0.00318	3	0.601	2	0.00611	0.01158	2	0.00611	0.01158	1	0.00096	0.00059
ES418315.1	23	0.01485	0.01701	10	0.866	14	0.04387	0.05512	14	0.04387	0.05512	9	0.00757	0.00713
ES418915.1	4	0.00270	0.00282	4	0.621	4	0.00330	0.00345	0	0.00000	0.00000	0	0.00000	0.00000
ES419198.1	6	0.00443	0.00487	4	0.581	5	0.00532	0.00667	0	0.00000	0.00000	1	0.00242	0.00078
ES419223.1	9	0.00561	0.00717	7	0.831	8	0.00763	0.01065	2	0.01455	0.02481	1	0.00181	0.00060
ES419242.1	1	0.00036	0.00028	2	0.233	1	0.00045	0.00034	0	0.00000	0.00000	0	0.00000	0.00000
ES419657.1	1	0.00072	0.00080	2	0.300	1	0.00115	0.00127	1	0.00797	0.00884	0	0.00000	0.00000
ES420171.1	3	0.00346	0.00111	3	0.170	2	0.00320	0.00103	1	0.01280	0.00410	1	0.00412	0.00132
ES420250.1	21	0.00653	0.00411	13	0.850	19	0.00935	0.00619	3	0.01012	0.00423	2	0.00168	0.00054
ES420603.1	16	0.01020	0.00491	10	0.727	12	0.01713	0.00719	6	0.02860	0.01460	4	0.00463	0.00250
ES420757.1	3	0.00132	0.00114	4	0.614	2	0.00154	0.00170	0	0.00000	0.00000	1	0.00104	0.00038
ES420771.1	5	0.00483	0.00315	5	0.663	4	0.00581	0.00423	0	0.00000	0.00000	1	0.00291	0.00103
ES420862.1	20	0.00860	0.01038	9	0.854	8	0.00716	0.00770	5	0.01542	0.01961	12	0.01006	0.01302
ES421219.1	14	0.00770	0.00713	7	0.697	5	0.01139	0.01265	5	0.01220	0.01355	9	0.00656	0.00540
ES421311.1	7	0.00267	0.00127	5	0.424	6	0.00312	0.00139	2	0.01067	0.00530	1	0.00143	0.00093
ES421603.1	7	0.00359	0.00130	4	0.320	7	0.00938	0.00340	4	0.01319	0.00423	0	0.00000	0.00000
ES421877.1	3	0.00156	0.00211	3	0.579	3	0.00498	0.00672	3	0.00800	0.01079	0	0.00000	0.00000
ES422367.1	29	0.00862	0.00748	10	0.925	28	0.01056	0.00899	2	0.01022	0.01527	1	0.00145	0.00192
ES424016.1	9	0.00630	0.00672	7	0.800	5	0.01055	0.01048	2	0.00725	0.00993	4	0.00419	0.00485
ES428620.1	6	0.00259	0.00223	5	0.684	6	0.00324	0.00279	0	0.00000	0.00000	0	0.00000	0.00000
Pm_CL135Contig1	13	0.00653	0.00679	7	0.964	11	0.00757	0.00759	1	0.00602	0.00390	2	0.00369	0.00462
Pm_CL1400Contig1	9	0.00647	0.00998	6	0.822	5	0.01022	0.01496	3	0.01070	0.01359	4	0.00435	0.00812
Pm_CL150Contig1	2	0.00191	0.00200	3	0.433	2	0.00826	0.00868	2	0.00826	0.00868	0	0.00000	0.00000
Pm_CL1692Contig1	10	0.00775	0.00920	6	0.736	8	0.02298	0.02769	8	0.02628	0.03167	2	0.00212	0.00236
Pm_CL1811Contig1	10	0.00471	0.00521	7	0.792	10	0.00771	0.00816	0	0.00000	0.00000	0	0.00000	0.00000
Pm_CL1814Contig1	4	0.00295	0.00354	4	0.557	3	0.00849	0.01115	3	0.00849	0.01115	1	0.00100	0.00088
Pm_CL1868Contig1	1	0.00070	0.00118	2	0.467	1	0.00097	0.00164	0	0.00000	0.00000	0	0.00000	0.00000
Pm_CL1982Contig1	0	0.00000	0.00000	1	0.000	0	0.00000	0.00000	0	0.00000	0.00000	0	0.00000	0.00000

Pm_CL1994Contig1	14	0.00456	0.00449	13	0.913	10	0.00702	0.00837	2	0.00426	0.00535	4	0.00245	0.00112
Pm_CL1997Contig1	5	0.00199	0.00127	6	0.557	5	0.00368	0.00233	3	0.01485	0.01085	0	0.00000	0.00000
Pm_CL1Contig2	21	0.01034	0.01212	5	0.700	21	0.01379	0.01616	1	0.00655	0.01087	0	0.00000	0.00000
Pm_CL2089Contig1	1	0.00068	0.00042	2	0.166	1	0.00100	0.00061	0	0.00000	0.00000	0	0.00000	0.00000
Pm_CL2133Contig1	3	0.00243	0.00270	2	0.300	0	0.00000	0.00000	0	0.00000	0.00000	3	0.00312	0.00346
Pm_CL214Contig1	5	0.00381	0.00393	8	0.844	2	0.00363	0.00266	0	0.00000	0.00000	3	0.00396	0.00488
Pm_CL2282Contig1	1	0.00078	0.00150	2	0.522	0	0.00000	0.00000	0	0.00000	0.00000	1	0.00102	0.00197
Pm_CL234Contig1	9	0.00350	0.00476	3	0.464	9	0.00475	0.00647	1	0.00530	0.00775	0	0.00000	0.00000
Pm_CL618Contig1	0	0.00000	0.00000	1	0.000	0	0.00000	0.00000	0	0.00000	0.00000	0	0.00000	0.00000
Pm_CL61Contig1	5	0.00382	0.00476	5	0.776	5	0.00498	0.00621	0	0.00000	0.00000	0	0.00000	0.00000
Pm_CL73Contig1	12	0.00754	0.00987	7	0.735	10	0.00927	0.01255	0	0.00000	0.00000	2	0.00390	0.00421
Pm_CL783Contig1	11	0.00743	0.00943	9	0.896	4	0.00902	0.01469	4	0.01184	0.01929	7	0.00680	0.00722
Pm_CL795Contig1	2	0.00132	0.00094	3	0.372	2	0.00317	0.00227	0	0.00000	0.00000	0	0.00000	0.00000
Pm_CL855Contig1	4	0.00275	0.00156	4	0.486	3	0.00646	0.00421	2	0.00625	0.00510	1	0.00100	0.00033
Pm_CL908Contig1	14	0.00821	0.00333	4	0.399	12	0.01485	0.00606	2	0.00718	0.00403	2	0.00223	0.00170
Pm_CL919Contig1	21	0.00791	0.00818	9	0.853	19	0.01034	0.01058	1	0.00393	0.00248	2	0.00248	0.00282
Pm_CL922Contig1	2	0.00127	0.00042	3	0.177	1	0.00161	0.00053	1	0.00328	0.00109	1	0.00105	0.00035
Pm_CL939Contig1	10	0.00636	0.00586	6	0.762	4	0.00652	0.00665	3	0.00964	0.01101	6	0.00631	0.0054
Pm_CL969Contig1	5	0.00335	0.00250	6	0.727	3	0.00377	0.00389	2	0.00979	0.01357	2	0.00289	0.00093
Pm_CL988Contig1	6	0.00297	0.00211	7	0.696	3	0.00298	0.00270	0	0.00000	0.00000	3	0.00299	0.00154
sM13Df243	6	0.00600	0.00626	6	0.778	4	0.01053	0.01227	0	0.00000	0.00000	2	0.00323	0.00257
sSPcDFD005F06506	9	0.00555	0.00355	7	0.805	9	0.00695	0.00445	0	0.00000	0.00000	0	0.00000	0.00000
sSPcDFD015C12212	0	0.00000	0.00000	1	0.000	0	0.00000	0.00000	0	0.00000	0.00000	0	0.00000	0.00000
sSPcDFD024D11311	4	0.00291	0.00166	5	0.545	4	0.01349	0.00768	4	0.01349	0.00768	0	0.00000	0.00000
sSPcDFD040B03103	6	0.00435	0.00273	6	0.645	6	0.00736	0.00461	3	0.01624	0.01008	0	0.00000	0.00000
sSPcDFE002A03003	11	0.00727	0.00644	4	0.682	7	0.01127	0.00906	3	0.01174	0.00591	4	0.00451	0.00465
sSPcDFE025C06206	13	0.00937	0.00952	4	0.769	7	0.00851	0.00832	1	0.00576	0.00504	6	0.01104	0.01172
sSPcDFE028B10110	8	0.00509	0.00406	6	0.589	5	0.01224	0.01121	5	0.01613	0.01476	3	0.0026	0.00156
sSPcDFE038D06306	8	0.00634	0.00398	8	0.759	7	0.02452	0.01673	7	0.02492	0.01673	1	0.00102	0.00033
sSPcDFE044F10510	6	0.00508	0.00316	6	0.648	6	0.02067	0.01286	6	0.02067	0.01286	0	0.00000	0.00000

sSPcDFE049B06106	1	0.00078	0.00027	2	0.095	1	0.00220	0.00075	1	0.00452	0.00155	0	0.00000	0.00000
sSPcDFE049E11411	4	0.00277	0.00273	3	0.416	2	0.00345	0.00268	1	0.00361	0.00431	2	0.00232	0.00277
sSPcDFF014F08508	2	0.00129	0.00113	2	0.282	1	0.00117	0.00103	0	0.00000	0.00000	1	0.00145	0.00127
sSPcDFF015H05705	10	0.00947	0.00815	11	0.810	4	0.01370	0.01349	4	0.01774	0.01747	6	0.00789	0.00614
sSPcDFF044H10710	9	0.00402	0.00434	5	0.650	9	0.00517	0.00557	1	0.00567	0.00235	0	0.00000	0.00000
U22458.1	0	0.00000	0.00000	1	0.000	0	0.00000	0.00000	0	0.00000	0.00000	0	0.00000	0.00000
Z49715.1	28	0.00884	0.00928	13	0.947	26	0.01290	0.01370	2	0.00635	0.00415	2	0.00201	0.00132
Total	933			657		732			254			201		
Average	8	0.00450	0.00435	5	0.585	6	0.00777	0.00756	2	0.00791	0.00760	2	0.00214	0.00200
SD	7	0.00331	0.00358	3	0.262	6	0.00677	0.00765	2	0.00821	0.00901	2	0.00281	0.00297

Sites were categorized using the method of NEI AND GOJOBORI (1986). Estimates of nucleotide diversity are relative to length of aligned sequence, ignoring indels, for each candidate gene or interval.

[a]S = number of segregating sites.

[b]θ_W = Watterson's estimator of Θ.

[c]θ_π = Estimator of Θ from the average number of pairwise sequence differences.

[d]h = The number of haplotypes.

[e]H_d = Haplotypic diversity or the expected heterozygosity given the number of haplotypes (h) and their frequencies.

TABLE S6

Common measures of sequence divergence for 121 candidate genes

Locus	D_{xy}[a]	Ksil[b]	Ks[c]	Ka[d]	Ka/Ks	Ka/Ksil	$\theta_{\pi a}/\theta_{\pi s}$[e]	$\theta_{\pi a}/\theta_{\pi sil}$[e]
CD028057.1	0.01064	0.01516	0.04681	0.00372	0.07947	0.24538	na	0.00000
CN634517.1	0.00645	0.00909	0.01673	0.00454	0.27137	0.49945	0.04578	0.11047
CN634677.1	0.01434	0.00176	0.00176	0.01898	10.78409	10.78409	0.00000	0.00000
CN635137.1	0.01477	0.02001	0.01479	0.00224	0.15145	0.11194	0.15545	0.25021
CN635490.1	0.00878	0.00893	0.00458	0.00847	1.84934	0.94849	0.26561	0.66361
CN635596.1	0.01803	0.01539	0.02441	0.02095	0.85825	1.36127	0.09414	0.19158
CN635661.1	0.02438	0.02322	0.04721	0.02584	0.54734	1.11283	0.00000	0.00000
CN635674.1	0.00581	0.00165	0.00165	0.00704	4.26667	4.26667	3.09697	3.09697
CN635691.1	0.00660	0.01207	0.01235	0.00017	0.01377	0.01408	na	1.30769
CN636014.1	0.00747	0.02765	0.02765	0.00190	0.06872	0.06872	0.00000	0.00000
CN636043.1	0.00521	0.00444	0.00000	0.00845	na	1.90315	na	0.00000
CN636093.1	0.00785	0.00955	0.00000	0.00000	na	0.00000	na	0.00000
CN636149.1	0.00994	0.02252	0.01961	0.00029	0.01479	0.01288	na	0.04911
CN636303.1	0.00161	0.00231	0.00000	0.00000	na	0.00000	na	0.00000
CN636471.1	0.01369	0.03943	0.03943	0.00584	0.14811	0.14811	0.17101	0.17101
CN636492.1	0.01006	0.00904	0.00000	0.01145	na	1.26659	na	0.00000
CN636784.1	0.00285	0.01150	0.01150	0.00007	0.00609	0.00609	0.01889	0.01889
CN636795.1	0.00709	0.00881	0.00973	0.00469	0.48201	0.53235	0.13911	0.17784
CN636901.1	0.01803	0.02023	0.03727	0.00900	0.24148	0.44488	na	0.00000
CN636999.1	0.00000	0.00000	0.00000	0.00000	na	na	na	na
CN637166.1	0.00138	0.00406	0.00406	0.00053	0.13054	0.13054	0.12760	0.12760
CN637226.1	0.01606	0.04335	0.04335	0.00778	0.17947	0.17947	0.30229	0.30229
CN637244.1	0.01286	0.01073	0.01452	0.01469	1.01171	1.36906	0.00000	0.00000
CN637306.1	0.00928	0.00676	0.00561	0.01530	2.72727	2.26331	0.04374	0.05075

A. J. Eckert *et al.*

CN637339.1	0.01646	0.02931	0.03728	0.00502	0.13466	0.17127	0.31315	0.39856
CN637910.1	0.00344	0.01441	0.01441	0.00000	0.00000	0.00000	0.00000	0.00000
CN637944.1	0.00717	0.02107	0.02107	0.00258	0.12245	0.12245	0.35779	0.35779
CN638015.1	0.01842	0.01391	0.02755	0.02805	1.01815	2.01653	0.36661	0.44740
CN638070.1	0.01486	0.00686	0.00686	0.02040	2.97376	2.97376	0.66073	0.66073
CN638367.1	0.00187	0.00236	0.00131	0.00055	0.41985	0.23305	0.40000	0.63694
CN638381.1	0.00235	0.00083	0.00131	0.00304	2.32061	3.66265	0.00000	0.00000
CN638489.1	0.00469	0.01133	0.01723	0.00000	0.00000	0.00000	0.00000	0.00000
CN638545.1	0.00195	0.00465	0.00303	0.00000	0.00000	0.00000	0.00000	0.00000
CN638556.1	0.02838	0.04430	0.04430	0.02392	0.53995	0.53995	0.00000	0.00000
CN638735.1	0.00241	0.00114	0.00000	0.00473	na	4.14912	na	0.00000
CN639074.1	0.00792	0.00926	0.00000	0.00528	na	0.57019	na	0.26437
CN639087.1	0.00012	0.00051	0.00051	0.00000	0.00000	0.00000	0.00000	0.00000
CN639130.1	0.01140	0.00000	0.00000	0.01544	na	na	na	na
CN639236.1	0.00974	0.02262	0.02262	0.00563	0.24889	0.24889	0.07970	0.07970
CN639311.1	0.00777	0.00968	0.00000	0.00029	na	0.02996	na	2.00000
CN639346.1	0.00283	0.00610	0.00000	0.00000	na	0.00000	na	0.00000
CN639480.1	0.00711	0.01863	0.01863	0.00640	0.34353	0.34353	0.25089	0.25089
CN640037.1	0.00635	0.01359	0.02147	0.00377	0.17559	0.27741	2.92775	2.00198
CN640110.1	0.00824	0.02163	0.02163	0.00400	0.18493	0.18493	0.32447	0.32447
CN640155.1	0.00417	0.00102	0.00102	0.00504	4.94118	4.94118	0.51707	0.51707
CN640247.1	0.00382	0.00635	0.00378	0.00429	1.13492	0.67559	0.00000	0.00000
CN640289.1	0.00782	0.02187	0.03425	0.00240	0.07007	0.10974	0.24878	0.38953
CN640361.1	0.01309	0.01501	0.03838	0.00671	0.17483	0.44704	0.00000	0.00000
CN640419.1	0.00420	0.00699	0.00000	0.00000	na	0.00000	na	0.00000
CN640485.1	0.00827	0.01254	0.00335	0.00196	0.58507	0.15630	0.57440	0.89082
CN640493.1	0.00177	0.00043	0.00000	0.00378	na	8.79070	na	7.51765
CN640521.1	0.00582	0.01876	0.01876	0.00238	0.12687	0.12687	0.27005	0.27005
CN640670.1	0.00508	0.02135	0.02135	0.00000	0.00000	0.00000	na	na
CN640738.1	0.01423	0.01559	0.01295	0.01153	0.89035	0.73958	0.61173	0.63780

CN641116.1	0.00603	0.00849	0.00260	0.00000	0.00000	0.00000	0.00000	0.00000
CN641171.1	0.00812	0.01762	0.02579	0.00118	0.04575	0.06697	0.41320	0.35729
CN641226.1	0.00591	0.02401	0.02401	0.00031	0.01291	0.01291	0.05095	0.05095
ES418315.1	0.02246	0.06360	0.06360	0.01548	0.24340	0.24340	0.12935	0.12935
ES418915.1	0.00542	0.00663	0.00000	0.00000	na	0.00000	na	0.00000
ES419198.1	0.00379	0.00529	0.00000	0.00039	na	0.07372	na	0.11694
ES419223.1	0.00919	0.01065	0.02170	0.00030	0.01382	0.02817	0.02418	0.05634
ES419242.1	0.00376	0.00462	0.00000	0.00000	na	0.00000	na	0.00000
ES419657.1	0.00311	0.00497	0.00512	0.00000	0.00000	0.00000	0.00000	0.00000
ES420171.1	0.01295	0.01773	0.00205	0.00066	0.32195	0.03723	0.32195	1.28155
ES420250.1	0.00983	0.01359	0.02490	0.00338	0.13574	0.24871	0.12766	0.08724
ES420603.1	0.00430	0.00802	0.00765	0.00130	0.16993	0.16209	0.17123	0.34771
ES420757.1	0.00252	0.00426	0.01304	0.00019	0.01457	0.04460	na	0.22353
ES420771.1	0.00257	0.00360	0.00000	0.00052	na	0.14444	na	0.24350
ES420862.1	0.01125	0.01148	0.01979	0.01117	0.56443	0.97300	0.66395	1.69091
ES421219.1	0.00656	0.00906	0.00970	0.00579	0.59691	0.63907	0.39852	0.42688
ES421311.1	0.00340	0.00258	0.00274	0.00567	2.06934	2.19767	0.17547	0.66906
ES421603.1	0.00066	0.00172	0.00212	0.00000	0.00000	0.00000	0.00000	0.00000
ES421877.1	0.00545	0.01741	0.02795	0.00000	0.00000	0.00000	0.00000	0.00000
ES422367.1	0.00925	0.01080	0.01060	0.00360	0.33962	0.33333	0.12574	0.21357
ES424016.1	0.00924	0.02169	0.01924	0.00305	0.15852	0.14062	0.48842	0.46279
ES428620.1	0.00446	0.00558	0.00000	0.00000	na	0.00000	na	0.00000
Pm_CL135Contig1	0.01465	0.01272	0.00975	0.01975	2.02564	1.55267	1.18462	0.60870
Pm_CL1400Contig1	0.01096	0.01294	0.01043	0.01237	1.18600	0.95595	0.59750	0.54278
Pm_CL150Contig1	0.00119	0.00514	0.00514	0.00000	0.00000	0.00000	0.00000	0.00000
Pm_CL1692Contig1	0.00719	0.02142	0.02449	0.00194	0.07922	0.09057	0.07452	0.08523
Pm_CL1811Contig1	0.00801	0.01039	0.00000	0.00581	na	0.55919	na	0.00000
Pm_CL1814Contig1	0.00307	0.01045	0.01045	0.00048	0.04593	0.04593	0.07892	0.07892
Pm_CL1868Contig1	0.00168	0.00234	0.00000	0.00000	na	0.00000	na	0.00000
Pm_CL1982Contig1	0.00000	0.00000	0.00000	0.00000	na	na	na	na

Pm_CL1994Contig1	0.00832	0.01723	0.01437	0.00059	0.04106	0.03424	0.20935	0.13381
Pm_CL1997Contig1	0.00456	0.00775	0.03646	0.00000	0.00000	0.00000	0.00000	0.00000
Pm_CL1Contig2	0.01328	0.01770	0.00815	0.00000	0.00000	0.00000	0.00000	0.00000
Pm_CL2089Contig1	0.00478	0.00705	0.00000	0.00000	na	0.00000	na	0.00000
Pm_CL2133Contig1	0.00755	0.00000	0.00000	0.00969	na	na	na	na
Pm_CL214Contig1	0.00568	0.00571	0.00000	0.00569	na	0.99650	na	1.83459
Pm_CL2282Contig1	0.01000	0.01257	0.01257	0.00940	0.74781	0.74781	na	na
Pm_CL234Contig1	0.01656	0.01854	0.04511	0.00000	0.00000	0.00000	0.00000	0.00000
Pm_CL618Contig1	0.01974	0.01978	0.06210	0.02031	0.32705	1.02679	na	na
Pm_CL61Contig1	0.03441	0.02697	0.03569	0.06025	1.68815	2.23396	na	0.00000
Pm_CL73Contig1	0.01745	0.02351	0.04528	0.00471	0.10402	0.20034	na	0.33546
Pm_CL783Contig1	0.00918	0.01083	0.01422	0.00858	0.60338	0.79224	0.37429	0.49149
Pm_CL795Contig1	0.00212	0.00509	0.00000	0.00000	na	0.00000	na	0.00000
Pm_CL855Contig1	0.00342	0.00242	0.00301	0.00390	1.29568	1.61157	0.06471	0.07838
Pm_CL908Contig1	0.02946	0.04586	0.02469	0.01831	0.74160	0.39926	0.42184	0.28053
Pm_CL919Contig1	0.01442	0.01885	0.01562	0.00452	0.28937	0.23979	1.13710	0.26654
Pm_CL922Contig1	0.00483	0.00027	0.00054	0.00782	14.48148	28.96296	0.32110	0.66038
Pm_CL939Contig1	0.00588	0.00447	0.00770	0.00684	0.88831	1.53020	0.49046	0.81203
Pm_CL969Contig1	0.00667	0.00747	0.02829	0.00579	0.20467	0.77510	0.06853	0.23907
Pm_CL988Contig1	0.00453	0.00526	0.01270	0.00383	0.30157	0.72814	na	0.57037
sM13Df243	0.00902	0.01211	0.00000	0.00712	na	0.58794	na	0.20945
sSPcDFD005F06506	0.01552	0.01667	0.00000	0.01097	na	0.65807	na	0.00000
sSPcDFD015C12212	0.00000	0.00000	0.00000	0.00000	na	na	na	na
sSPcDFD024D11311	0.00900	0.01678	0.01678	0.00686	0.40882	0.40882	0.00000	0.00000
sSPcDFD040B03103	0.01203	0.02032	0.00538	0.00000	0.00000	0.00000	0.00000	0.00000
sSPcDFE002A03003	0.00815	0.01499	0.01280	0.00341	0.26641	0.22748	0.78680	0.51325
sSPcDFE025C06206	0.02478	0.03049	0.03850	0.01714	0.44519	0.56215	2.32540	1.40865
sSPcDFE028B10110	0.00928	0.02434	0.03207	0.00402	0.12535	0.16516	0.10569	0.13916
sSPcDFE038D06306	0.01398	0.02285	0.02285	0.01145	0.50109	0.50109	0.01973	0.01973
sSPcDFE044F10510	0.00557	0.02266	0.02266	0.00000	0.00000	0.00000	0.00000	0.00000

sSPcDFE049B06106	0.00577	0.00828	0.00077	0.00460	5.97403	0.55556	0.00000	0.00000
sSPcDFE049E11411	0.00160	0.00153	0.00256	0.00165	0.64453	1.07843	0.64269	1.03358
sSPcDFF014F08508	0.00462	0.00784	0.00000	0.00069	na	0.08801	na	1.23301
sSPcDFF015H05705	0.00532	0.00825	0.01068	0.00422	0.39513	0.51152	0.35146	0.45515
sSPcDFF044H10710	0.01604	0.01678	0.03882	0.01353	0.34853	0.80632	0.00000	0.00000
U22458.1	0.00992	0.01870	0.01870	0.00735	0.39305	0.39305	na	na
Z49715.1	0.01523	0.01963	0.00226	0.00649	2.87168	0.33062	0.31807	0.09635
n	121	121	121	121	93	116	81	112
Average	0.00852	0.01296	0.01413	0.00580	0.88548	0.99037	0.30898	0.38079
SD	0.00619	0.01059	0.01498	0.00806	2.06162	3.02613	0.55467	0.85179

Sites were categorized using the method of NEI AND GOJOBORI (1986). Estimates of divergence are relative to length of aligned sequence, ignoring indels, for each candidate gene.

[a]D_{xy} = Pairwise sequence divergence between coastal and bigcone Douglas-fir.

[b]$Ksil$ = Pairwise sequence divergence at silent sites.

[c]Ks = Pairwise sequence divergence at synonymous sites.

[d]Ka = Pairwise sequence divergence at nonsynonymous sites.

[e]Measures of nucleotide diversity from Table S2.

TABLE S7

A summary of Markov chain Monte Carlo (MCMC) estimates of parameters for the instantaneous growth model

Model	Parameter Estimates		ESS[a]		Acceptance Rate (%)[b]
	f	τ	f	τ	
IGM	(0,0.99]	(0,0.10]			
MCMC replicate 1	0.604	0.039	137.2	85.7	31.7
	0.209-0.985	0.002-0.093			
MCMC replicate 2	0.666	0.039	160.9	90.5	31.4
	0.279-0.989	0.003-0.094			
MCMC replicate 3	0.730	0.045	146.2	90.6	32.4
	0.262-0.989	0.003-0.092			

Parameters were estimated from Markov chains that were run for 1.2×10^6 steps with the first 0.2×10^6 steps being discarded as burn-in. The joint posterior distribution of f and τ was processed using the kernel smoothing functions available in R. The set of parameter values that maximized the smoothed joint density was taken as the joint parameter estimate. Three independent MCMC simulations were run for each population growth model. Convergence was assessed through similarities between the resulting approximate posterior distributions (Fig. S2) and effective sample size (ESS) estimates calculated using the CODA v. 0.13-2 package in R.

[a]ESS = effective sample size of the MCMC samples.

[b]The acceptance rate is the number of proposals along the Markov chain which were accepted across the 18 genes analyzed by KRUTOVSKY AND NEALE (2005).

TABLE S8

Common measures of neutrality based on the folded site frequency spectrum or haplotype distributions for 121 candidate genes

Locus	D	P_{WF}	P_{IGM}	P_{BIM_100}	D^*	P_{WF}	P_{IGM}	P_{BIM_100}	F^*	P_{WF}	P_{IGM}	P_{BIM_100}	F_{obs}	P_{WF}	P_{IGM}	P_{BIM_100}
CD028057.1	1.026	0.792	0.796	0.815	0.650	0.402	0.405	0.423	0.857	0.721	0.728	0.732	0.580	0.719	0.738	0.755
CN634517.1	-1.530	0.036	0.058	0.072	-2.136	0.031	0.037	0.059	-2.272	0.033	0.056	0.077	0.463	0.033	0.035	0.042
CN634677.1	-0.213	0.493	0.523	0.528	0.629	0.380	0.399	0.400	0.461	0.488	0.499	0.523	0.773	0.434	0.453	0.470
CN635137.1	-0.166	0.558	0.563	0.584	-0.381	0.315	0.328	0.353	-0.369	0.345	0.365	0.388	0.102	0.032	0.040	0.045
CN635490.1	-0.280	0.486	0.509	0.529	0.344	0.556	0.578	0.590	0.192	0.522	0.532	0.559	0.474	0.427	0.451	0.466
CN635596.1	-0.893	0.248	0.256	0.263	-0.128	0.420	0.430	0.446	-0.415	0.341	0.362	0.366	0.357	0.080	0.082	0.094
CN635661.1	1.917	0.983	0.991	0.996	1.006	0.832	0.857	0.864	1.444	0.965	0.994	1.000	0.460	0.715	0.725	0.747
CN635674.1	-0.591	0.359	0.360	0.379	-1.514	0.090	0.108	0.132	-1.449	0.121	0.144	0.150	0.418	0.297	0.306	0.309
CN635691.1	-1.515	0.012	0.018	0.036	-2.135	0.015	0.021	0.027	-2.260	0.016	0.026	0.030	0.837	<0.001	0.002	0.009
CN636014.1	0.203	0.672	0.674	0.685	0.629	0.712	0.737	0.745	0.586	0.694	0.709	0.723	0.357	0.606	0.622	0.625
CN636043.1	-0.412	0.443	0.454	0.469	0.216	0.564	0.576	0.597	0.030	0.496	0.505	0.505	0.157	0.682	0.697	0.706
CN636093.1	0.593	0.695	0.699	0.706	0.635	0.397	0.415	0.419	0.715	0.639	0.654	0.658	0.648	0.620	0.636	0.647
CN636149.1	0.862	0.841	0.849	0.878	0.420	0.598	0.611	0.634	0.623	0.683	0.697	0.718	0.216	0.172	0.195	0.203
CN636303.1	-1.161	0.304	0.333	0.354	-1.591	0.038	0.045	0.054	-1.692	0.038	0.051	0.079	0.917	<0.001	0.009	0.015
CN636471.1	0.256	0.702	0.726	0.736	0.089	0.500	0.503	0.529	0.162	0.541	0.556	0.577	0.187	0.296	0.308	0.334
CN636492.1	-0.681	0.324	0.328	0.351	0.623	0.380	0.410	0.433	0.310	0.375	0.401	0.425	0.847	0.273	0.290	0.310
CN636784.1	-1.193	0.152	0.159	0.180	-0.811	0.213	0.221	0.249	-1.075	0.169	0.172	0.176	0.479	0.031	0.054	0.077
CN636795.1	0.273	0.713	0.732	0.751	-0.159	0.406	0.429	0.449	-0.034	0.476	0.503	0.512	0.187	0.529	0.538	0.555
CN636901.1	1.702	0.970	0.977	1.000	1.236	0.933	0.955	0.968	1.588	0.976	0.979	0.993	0.312	0.903	0.932	0.959
CN636999.1	na	na	na	na	na	na	na	na	na	na	na	na	na	na	na	na
CN637166.1	-0.987	0.258	0.286	0.303	0.254	0.520	0.532	0.535	-0.089	0.433	0.453	0.482	0.586	0.052	0.077	0.084
CN637226.1	1.524	0.949	0.952	0.978	1.249	0.936	0.956	0.974	1.532	0.969	0.992	0.999	0.165	0.981	0.989	0.994
CN637244.1	0.072	0.616	0.623	0.635	-0.198	0.354	0.375	0.389	-0.140	0.420	0.431	0.447	0.335	0.259	0.281	0.308
CN637306.1	-0.578	0.369	0.384	0.411	0.956	0.872	0.889	0.898	0.575	0.713	0.718	0.725	0.187	0.617	0.645	0.650
CN637339.1	-0.003	0.617	0.636	0.666	-0.173	0.396	0.423	0.432	-0.142	0.428	0.433	0.459	0.211	0.424	0.431	0.449

A. J. Eckert *et al.*

CN637910.1	0.028	0.603	0.621	0.630	0.344	0.566	0.588	0.589	0.294	0.568	0.584	0.589	0.206	0.650	0.674	0.687
CN637944.1	-0.963	0.224	0.229	0.232	-0.354	0.341	0.361	0.380	-0.611	0.277	0.278	0.290	0.225	0.327	0.348	0.374
CN638015.1	-0.712	0.315	0.318	0.329	-0.081	0.439	0.445	0.452	-0.308	0.370	0.377	0.385	0.229	0.477	0.479	0.480
CN638070.1	-0.498	0.387	0.396	0.420	-0.504	0.292	0.318	0.331	-0.569	0.309	0.309	0.338	0.389	0.056	0.071	0.083
CN638367.1	-1.616	0.046	0.054	0.059	-0.782	0.213	0.216	0.244	-1.193	0.142	0.167	0.184	0.505	0.036	0.058	0.077
CN638381.1	0.650	0.718	0.723	0.737	0.688	0.442	0.445	0.470	0.772	0.645	0.668	0.691	0.625	0.624	0.632	0.644
CN638489.1	-0.240	0.494	0.496	0.501	-0.955	0.178	0.193	0.195	-0.873	0.226	0.236	0.256	0.289	0.149	0.169	0.191
CN638545.1	-0.328	0.472	0.491	0.509	0.639	0.710	0.723	0.726	0.416	0.623	0.641	0.663	0.478	0.098	0.104	0.107
CN638556.1	1.577	0.954	0.974	0.996	0.844	0.719	0.734	0.757	1.202	0.927	0.940	0.949	0.365	0.954	0.957	0.962
CN638735.1	1.533	0.933	0.947	0.950	0.629	0.385	0.412	0.428	1.000	0.872	0.881	0.894	0.509	0.906	0.911	0.914
CN639074.1	-0.903	0.252	0.272	0.298	-0.856	0.186	0.208	0.228	-1.005	0.191	0.211	0.220	0.413	0.242	0.266	0.295
CN639087.1	-1.161	0.290	0.312	0.338	-1.591	0.039	0.040	0.068	-1.692	0.039	0.046	0.058	0.917	<0.001	na	na
CN639130.1	1.564	0.955	0.983	0.985	0.858	0.720	0.737	0.763	1.206	0.921	0.935	0.952	0.556	0.781	0.792	0.800
CN639236.1	0.466	0.744	0.762	0.767	0.674	0.725	0.740	0.761	0.711	0.729	0.741	0.764	0.125	0.863	0.876	0.879
CN639311.1	-1.729	0.007	0.026	0.026	-2.460	0.006	0.035	0.064	-2.601	0.006	0.033	0.059	0.752	<0.001	na	na
CN639346.1	0.125	0.591	0.592	0.619	1.033	0.850	0.862	0.881	0.905	0.759	0.770	0.772	0.709	0.482	0.501	0.505
CN639480.1	0.221	0.679	0.690	0.696	-0.243	0.355	0.375	0.378	-0.124	0.430	0.453	0.466	0.236	0.241	0.271	0.291
CN640037.1	-0.605	0.354	0.366	0.372	-1.139	0.138	0.159	0.186	-1.142	0.154	0.158	0.159	0.054	0.122	0.130	0.143
CN640110.1	-0.864	0.298	0.300	0.321	0.844	0.724	0.747	0.763	0.431	0.530	0.539	0.545	0.841	0.279	0.280	0.310
CN640155.1	-1.706	0.009	0.035	0.064	-2.255	0.011	0.038	0.049	-2.414	0.011	0.017	0.028	0.785	<0.001	0.008	0.021
CN640247.1	-0.826	0.283	0.288	0.298	-1.649	0.078	0.107	0.121	-1.636	0.086	0.101	0.104	0.493	0.089	0.111	0.128
CN640289.1	1.870	0.981	0.994	0.995	0.844	0.719	0.734	0.752	1.294	0.952	0.979	0.997	0.274	0.981	0.993	1.000
CN640361.1	1.345	0.954	0.966	0.991	1.072	0.916	0.916	0.942	1.346	0.948	0.950	0.953	0.116	0.663	0.686	0.697
CN640419.1	1.479	0.934	0.939	0.946	1.095	0.882	0.890	0.900	1.389	0.952	0.955	0.972	0.442	0.827	0.854	0.883
CN640485.1	-0.570	0.372	0.379	0.390	-1.022	0.161	0.163	0.180	-1.034	0.177	0.201	0.228	0.183	0.683	0.707	0.726
CN640493.1	-0.467	0.400	0.412	0.423	-0.039	0.404	0.424	0.433	-0.174	0.418	0.423	0.447	0.508	0.249	0.271	0.276
CN640521.1	0.675	0.802	0.815	0.822	0.509	0.636	0.642	0.669	0.645	0.703	0.728	0.728	0.391	0.518	0.539	0.551
CN640670.1	na	na	na	na	na	na	na	na	na	na	na	na	na	na	na	na
CN640738.1	0.513	0.796	0.807	0.810	0.356	0.619	0.629	0.639	0.469	0.671	0.673	0.674	0.143	0.564	0.580	0.599
CN641116.1	-0.261	0.518	0.525	0.525	-0.014	0.469	0.474	0.498	-0.104	0.442	0.443	0.461	0.247	0.353	0.381	0.396
CN641171.1	-0.474	0.418	0.418	0.447	1.240	0.938	0.962	0.973	0.868	0.779	0.793	0.807	0.409	0.459	0.485	0.511
CN641226.1	1.195	0.891	0.916	0.925	0.986	0.824	0.828	0.856	1.204	0.901	0.930	0.944	0.425	0.762	0.791	0.820

ES418315.1	0.549	0.811	0.828	0.834	0.641	0.753	0.760	0.769	0.715	0.777	0.799	0.800	0.174	0.224	0.243	0.267
ES418915.1	0.119	0.622	0.649	0.670	0.128	0.459	0.469	0.473	0.145	0.498	0.527	0.552	0.406	0.569	0.575	0.577
ES419198.1	0.303	0.702	0.720	0.737	-0.946	0.175	0.196	0.225	-0.680	0.266	0.276	0.277	0.444	0.286	0.299	0.313
ES419223.1	0.933	0.867	0.868	0.889	-0.220	0.356	0.365	0.393	0.134	0.526	0.532	0.560	0.207	0.657	0.677	0.703
ES419242.1	-0.448	0.388	0.389	0.417	0.688	0.447	0.450	0.473	0.450	0.444	0.445	0.469	0.781	0.323	0.350	0.368
ES419657.1	0.186	0.595	0.598	0.602	0.629	0.394	0.417	0.420	0.584	0.562	0.585	0.600	0.713	0.537	0.565	0.592
ES420171.1	-1.731	0.006	0.032	0.036	-2.494	0.007	0.035	0.060	-2.631	0.007	0.014	0.034	0.837	<0.001	0.012	0.017
ES420250.1	-1.370	0.090	0.094	0.099	-1.907	0.052	0.069	0.093	-2.037	0.052	0.054	0.055	0.187	0.008	0.028	0.030
ES420603.1	-1.864	0.020	0.035	0.061	-1.521	0.088	0.115	0.125	-1.894	0.063	0.065	0.070	0.304	0.004	0.016	0.031
ES420757.1	-0.385	0.464	0.469	0.481	-1.225	0.148	0.155	0.156	-1.145	0.192	0.208	0.234	0.418	0.301	0.331	0.334
ES420771.1	-1.060	0.226	0.244	0.251	-2.012	0.047	0.071	0.072	-2.015	0.056	0.081	0.093	0.370	0.179	0.183	0.198
ES420862.1	0.760	0.855	0.869	0.882	-0.376	0.319	0.332	0.350	-0.038	0.468	0.496	0.503	0.183	0.354	0.379	0.381
ES421219.1	-0.263	0.504	0.521	0.529	1.131	0.914	0.944	0.953	0.836	0.803	0.814	0.842	0.335	0.269	0.274	0.277
ES421311.1	-1.703	0.033	0.058	0.063	-1.242	0.134	0.152	0.166	-1.590	0.102	0.104	0.111	0.596	0.015	0.028	0.033
ES421603.1	-2.015	0.003	0.022	0.046	-2.614	0.012	0.017	0.042	-2.831	0.012	0.033	0.033	0.694	0.032	0.037	0.042
ES421877.1	0.949	0.831	0.849	0.874	-0.105	0.372	0.392	0.407	0.208	0.493	0.522	0.531	0.452	0.591	0.618	0.638
ES422367.1	-0.546	0.376	0.390	0.415	-0.986	0.167	0.178	0.202	-0.995	0.181	0.182	0.187	0.133	0.414	0.442	0.468
ES424016.1	0.224	0.678	0.703	0.733	-0.196	0.369	0.379	0.379	-0.086	0.445	0.460	0.462	0.238	0.297	0.313	0.321
ES428620.1	-0.464	0.405	0.428	0.437	-1.418	0.120	0.134	0.139	-1.330	0.148	0.157	0.173	0.356	0.215	0.217	0.239
Pm_CL135Contig1	0.203	0.618	0.644	0.667	0.196	0.561	0.574	0.593	0.219	0.568	0.580	0.584	0.156	<0.001	0.009	0.018
Pm_CL1400Contig1	1.799	0.978	1.000	1.000	1.374	0.970	0.986	0.989	1.742	0.988	0.999	1.000	0.214	0.958	0.975	0.990
Pm_CL150Contig1	0.130	0.563	0.588	0.618	0.907	0.744	0.757	0.757	0.803	0.665	0.679	0.702	0.594	0.437	0.442	0.464
Pm_CL1692Contig1	0.637	0.816	0.842	0.845	-0.062	0.442	0.450	0.474	0.165	0.541	0.554	0.563	0.298	0.334	0.336	0.346
Pm_CL1811Contig1	0.396	0.719	0.728	0.738	0.094	0.494	0.498	0.499	0.204	0.549	0.564	0.584	0.258	0.161	0.189	0.198
Pm_CL1814Contig1	0.564	0.756	0.756	0.765	1.090	0.877	0.890	0.901	1.088	0.862	0.870	0.890	0.467	0.641	0.664	0.679
Pm_CL1868Contig1	1.202	0.834	0.840	0.868	0.642	0.418	0.426	0.440	0.906	0.776	0.777	0.781	0.556	0.783	0.792	0.821
Pm_CL1982Contig1	na	na	na	na	na	na	na	na	na	na	na	na	na	na	na	na
Pm_CL1994Contig1	-0.058	0.587	0.612	0.637	-0.773	0.209	0.232	0.239	-0.652	0.259	0.263	0.270	0.127	0.161	0.184	0.205
Pm_CL1997Contig1	-1.093	0.217	0.243	0.259	-0.438	0.313	0.328	0.358	-0.719	0.258	0.271	0.293	0.469	0.051	0.054	0.074
Pm_CL1Contig2	0.694	0.829	0.858	0.870	1.106	0.926	0.951	0.959	1.142	0.907	0.925	0.939	0.344	0.245	0.255	0.259
Pm_CL2089Contig1	-0.662	0.336	0.337	0.365	0.629	0.387	0.401	0.410	0.323	0.382	0.403	0.411	0.841	0.277	0.280	0.293
Pm_CL2133Contig1	0.277	0.689	0.693	0.714	0.986	0.822	0.823	0.846	0.909	0.775	0.778	0.802	0.713	0.538	0.554	0.571

Pm_CL214Contig1	0.095	0.622	0.647	0.655	-0.461	0.305	0.312	0.320	-0.350	0.362	0.387	0.413	0.194	0.590	0.592	0.619
Pm_CL2282Contig1	1.583	0.975	0.982	0.996	0.629	0.390	0.391	0.395	1.015	0.897	0.911	0.912	0.501	0.955	0.965	0.972
Pm_CL234Contig1	1.280	0.928	0.935	0.940	1.383	0.970	0.986	0.992	1.563	0.969	0.981	0.989	0.562	0.619	0.620	0.639
Pm_CL618Contig1	na	na	na	na	na	na	na	na	na	na	na	na	na	na	na	na
Pm_CL61Contig1	0.745	0.809	0.834	0.841	0.372	0.578	0.584	0.587	0.551	0.656	0.682	0.695	0.261	0.816	0.837	0.842
Pm_CL73Contig1	1.068	0.904	0.927	0.932	0.602	0.721	0.741	0.750	0.862	0.813	0.838	0.868	0.297	0.253	0.280	0.302
Pm_CL783Contig1	0.928	0.877	0.897	0.905	1.437	0.985	0.997	1.000	1.497	0.963	0.973	0.981	0.145	0.863	0.886	0.913
Pm_CL795Contig1	-0.636	0.407	0.419	0.433	-0.646	0.218	0.222	0.250	-0.740	0.255	0.265	0.278	0.645	0.250	0.273	0.281
Pm_CL855Contig1	-1.194	0.114	0.130	0.144	-1.796	0.051	0.067	0.068	-1.879	0.061	0.088	0.091	0.535	0.173	0.200	0.220
Pm_CL908Contig1	-2.234	0.001	0.024	0.035	-3.019	0.003	0.024	0.041	-3.233	0.002	0.006	0.010	0.623	0.047	0.063	0.077
Pm_CL919Contig1	0.124	0.673	0.679	0.679	0.275	0.578	0.589	0.619	0.268	0.587	0.615	0.618	0.186	0.419	0.433	0.442
Pm_CL922Contig1	-1.515	0.015	0.041	0.060	-2.109	0.014	0.041	0.043	-2.238	0.015	0.029	0.037	0.831	<0.001	0.009	0.016
Pm_CL939Contig1	-0.270	0.495	0.498	0.522	0.926	0.836	0.860	0.873	0.672	0.737	0.759	0.779	0.274	0.534	0.551	0.572
Pm_CL969Contig1	-0.742	0.310	0.311	0.334	-1.309	0.102	0.115	0.124	-1.328	0.138	0.167	0.175	0.304	0.292	0.312	0.342
Pm_CL988Contig1	-0.888	0.256	0.257	0.278	0.509	0.636	0.664	0.688	0.124	0.517	0.539	0.544	0.335	0.104	0.132	0.161
sM13Df243	0.137	0.633	0.662	0.689	-0.130	0.387	0.405	0.424	-0.064	0.458	0.475	0.476	0.263	0.567	0.596	0.605
sSPcDFD005F06506	-1.223	0.129	0.144	0.158	-1.769	0.065	0.081	0.085	-1.868	0.067	0.096	0.114	0.503	0.766	0.772	0.791
sSPcDFD015C12212	na	na	na	na	na	na	na	na	na	na	na	na	na	na	na	na
sSPcDFD024D11311	-1.194	0.111	0.125	0.145	-1.796	0.058	0.060	0.078	-1.879	0.068	0.085	0.110	0.478	0.103	0.110	0.127
sSPcDFD040B03103	-1.159	0.174	0.185	0.210	0.521	0.636	0.647	0.664	0.047	0.484	0.492	0.512	0.384	0.348	0.369	0.385
sSPcDFE002A03003	-0.474	0.377	0.393	0.407	-1.106	0.160	0.170	0.183	-1.071	0.187	0.205	0.222	0.375	0.323	0.351	0.363
sSPcDFE025C06206	0.066	0.620	0.639	0.667	1.481	0.989	0.994	0.999	1.263	0.921	0.947	0.958	0.080	0.710	0.722	0.736
sSPcDFE028B10110	-0.667	0.338	0.361	0.375	-0.408	0.332	0.358	0.360	-0.560	0.299	0.314	0.334	0.438	0.096	0.103	0.111
sSPcDFE038D06306	-1.209	0.136	0.136	0.146	-1.022	0.165	0.174	0.184	-1.250	0.148	0.156	0.165	0.274	0.082	0.107	0.133
sSPcDFE044F10510	-1.155	0.185	0.211	0.228	-1.673	0.074	0.090	0.111	-1.766	0.075	0.102	0.117	0.380	0.147	0.149	0.176
sSPcDFE049B06106	-1.164	0.270	0.283	0.307	-1.558	0.040	0.066	0.091	-1.663	0.040	0.046	0.055	0.909	<0.001	0.005	0.012
sSPcDFE049E11411	-0.044	0.561	0.585	0.610	0.174	0.492	0.501	0.503	0.131	0.505	0.523	0.549	0.605	0.288	0.293	0.319
sSPcDFF014F08508	-0.350	0.418	0.430	0.441	0.953	0.775	0.775	0.801	0.705	0.635	0.662	0.671	0.740	0.349	0.367	0.377
sSPcDFF015H05705	-0.470	0.417	0.418	0.433	-1.077	0.145	0.156	0.156	-1.045	0.170	0.176	0.195	0.225	0.032	0.040	0.052
sSPcDFF044H10710	0.288	0.705	0.712	0.717	0.429	0.624	0.651	0.666	0.448	0.636	0.657	0.681	0.391	0.127	0.148	0.149
U22458.1	na	na	na	na	na	na	na	na	na	na	na	na	na	na	na	na
Z49715.1	0.194	0.693	0.710	0.713	-0.335	0.330	0.349	0.372	-0.207	0.394	0.415	0.443	0.100	0.480	0.495	0.513

Average	-0.142	-0.177	-0.194	0.416
SD	0.970	1.091	1.162	0.221

Probability values (P) corresponding to the left tail of the null distribution were derived from 10,000 coalescent simulations assuming a Wright-Fisher population (WF), an instantaneous growth model (IGM) and a bottleneck model with the timing of the bottleneck set at 100,000 yrs ago (BIM_100). P-values for the EW test are one minus the proportion of the null distribution to the left of the observed value. D = Tajima's D (TAJIMA 1989), D* = Fu and Li's D* (FU AND LI 1993), F* = Fu and Li's F* (FU AND LI 1993), F_{obs} = observed homozygosity from the Ewen-Watterson test (WATTERSON 1978) and SD = standard deviation.

TABLE S9

Common measures of neutrality based on the unfolded site frequency spectrum for 121 candidate genes

Locus	D_{fl}	P_{WF}	P_{IGM}	P_{BIM_100}	F	P_{WF}	P_{IGM}	P_{BIM_100}	H	P_{WF}	P_{IGM}	P_{BIM_100}	E	P_{WF}	P_{IGM}	P_{BIM_100}
CD028057.1	0.627	0.398	0.408	0.418	0.844	0.703	0.732	0.747	0.599	0.837	0.849	0.865	0.129	0.624	0.630	0.642
CN634517.1	-2.361	0.016	0.024	0.037	-2.504	0.019	0.036	0.060	-0.700	0.152	0.174	0.195	-0.470	0.403	0.416	0.420
CN634677.1	0.610	0.373	0.384	0.394	0.455	0.482	0.491	0.509	0.485	0.641	0.666	0.693	-0.515	0.403	0.405	0.409
CN635137.1	-0.554	0.301	0.318	0.319	-0.518	0.332	0.332	0.349	0.737	0.795	0.816	0.819	-0.873	0.228	0.235	0.245
CN635490.1	0.317	0.553	0.579	0.596	0.168	0.531	0.550	0.563	0.877	0.953	0.955	0.973	-0.954	0.184	0.197	0.201
CN635596.1	-0.221	0.407	0.427	0.441	-0.523	0.325	0.355	0.376	-0.087	0.304	0.307	0.307	-0.629	0.321	0.327	0.339
CN635661.1	1.012	0.825	0.840	0.843	1.478	0.962	0.988	0.996	-1.338	0.096	0.105	0.115	2.384	0.982	0.991	0.995
CN635674.1	-1.752	0.068	0.085	0.102	-1.681	0.102	0.103	0.105	0.607	0.714	0.721	0.732	-0.962	0.185	0.191	0.204
CN635691.1	-2.245	0.010	0.031	0.059	-2.384	0.010	0.011	0.037	0.267	0.422	0.450	0.468	-1.182	0.065	0.071	0.079
CN636014.1	0.632	0.696	0.715	0.716	0.597	0.682	0.686	0.712	-1.633	0.063	0.085	0.113	1.591	0.946	0.952	0.953
CN636043.1	0.170	0.561	0.576	0.589	-0.030	0.496	0.504	0.516	0.720	0.777	0.801	0.822	-1.073	0.168	0.172	0.173
CN636093.1	0.615	0.382	0.385	0.386	0.705	0.640	0.653	0.666	-2.116	0.055	0.073	0.085	2.046	0.955	0.965	0.973
CN636149.1	0.389	0.590	0.619	0.640	0.618	0.676	0.681	0.692	0.646	0.759	0.787	0.796	0.025	0.583	0.597	0.599
CN636303.1	-1.640	0.031	0.037	0.054	-1.751	0.032	0.039	0.066	0.200	0.251	0.269	0.291	-0.863	0.275	0.284	0.286
CN636471.1	0.027	0.491	0.496	0.512	0.121	0.535	0.562	0.572	-1.373	0.077	0.093	0.108	1.504	0.943	0.953	0.968
CN636492.1	0.605	0.385	0.386	0.410	0.306	0.389	0.402	0.405	0.351	0.481	0.499	0.528	-0.693	0.304	0.312	0.317
CN636784.1	-0.969	0.182	0.196	0.211	-1.240	0.159	0.181	0.192	0.212	0.402	0.421	0.424	-1.096	0.146	0.150	0.158
CN636795.1	-0.263	0.396	0.416	0.440	-0.109	0.460	0.461	0.461	0.570	0.665	0.679	0.688	-0.319	0.450	0.456	0.460
CN636901.1	1.291	0.931	0.948	0.956	1.675	0.973	0.978	0.988	-1.359	0.086	0.111	0.132	2.413	0.987	0.999	1.000
CN636999.1	na	na	na	na	na	na	na	na	na	na	na	na	na	na	na	na
CN637166.1	0.199	0.516	0.543	0.570	-0.146	0.443	0.450	0.467	0.702	0.827	0.851	0.858	-1.273	0.063	0.066	0.077
CN637226.1	1.310	0.934	0.953	0.979	1.629	0.965	0.979	0.994	-0.439	0.210	0.222	0.249	1.477	0.929	0.943	0.947
CN637244.1	-0.279	0.355	0.367	0.389	-0.208	0.419	0.421	0.451	-0.120	0.282	0.308	0.313	0.157	0.636	0.643	0.650
CN637306.1	1.040	0.869	0.894	0.910	0.619	0.726	0.746	0.755	0.505	0.605	0.613	0.639	-0.962	0.193	0.194	0.207
CN637339.1	-0.294	0.397	0.418	0.442	-0.240	0.421	0.446	0.455	-0.572	0.183	0.183	0.200	0.557	0.774	0.787	0.791

CN637910.1	0.317	0.556	0.563	0.582	0.275	0.561	0.589	0.598	0.487	0.590	0.597	0.604	-0.401	0.441	0.455	0.464
CN637944.1	-0.475	0.327	0.334	0.348	-0.741	0.266	0.293	0.312	-0.218	0.254	0.273	0.299	-0.517	0.371	0.383	0.384
CN638015.1	0.278	0.579	0.581	0.597	-0.039	0.477	0.501	0.517	-0.422	0.209	0.216	0.225	-0.168	0.517	0.527	0.534
CN638070.1	-1.072	0.195	0.196	0.198	-1.172	0.188	0.205	0.209	0.806	0.896	0.899	0.902	-1.245	0.091	0.096	0.109
CN638367.1	-0.943	0.179	0.198	0.226	-1.374	0.131	0.153	0.171	0.645	0.742	0.748	0.760	-1.809	0.007	0.008	0.021
CN638381.1	0.657	0.419	0.445	0.470	0.758	0.637	0.652	0.656	0.616	0.908	0.920	0.937	-0.131	0.539	0.540	0.553
CN638489.1	-1.228	0.120	0.123	0.146	-1.130	0.190	0.201	0.206	0.478	0.586	0.595	0.614	-0.633	0.314	0.319	0.321
CN638545.1	0.643	0.709	0.714	0.718	0.417	0.628	0.650	0.655	0.902	0.955	0.971	0.977	-1.040	0.169	0.177	0.182
CN638556.1	0.834	0.718	0.744	0.757	1.207	0.916	0.926	0.943	0.343	0.477	0.485	0.490	0.724	0.777	0.787	0.791
CN638735.1	0.610	0.375	0.403	0.417	0.986	0.868	0.893	0.915	0.286	0.477	0.503	0.532	0.703	0.777	0.791	0.805
CN639074.1	0.073	0.455	0.467	0.492	-0.244	0.397	0.419	0.436	-1.393	0.087	0.110	0.118	0.560	0.747	0.759	0.769
CN639087.1	-1.640	0.035	0.041	0.046	-1.751	0.035	0.053	0.064	0.200	0.245	0.270	0.279	-0.863	0.265	0.272	0.285
CN639130.1	0.847	0.722	0.735	0.748	1.212	0.922	0.950	0.963	-1.483	0.086	0.115	0.135	2.205	0.967	0.977	0.989
CN639236.1	0.679	0.724	0.736	0.760	0.734	0.735	0.759	0.783	0.199	0.395	0.422	0.445	0.161	0.639	0.652	0.665
CN639311.1	-2.639	0.003	0.016	0.041	-2.795	0.004	0.027	0.057	0.321	0.462	0.483	0.501	-1.409	0.025	0.038	0.050
CN639346.1	1.039	0.835	0.848	0.875	0.931	0.758	0.782	0.799	0.872	0.968	0.983	0.995	-0.667	0.322	0.332	0.343
CN639480.1	0.110	0.524	0.545	0.557	0.279	0.585	0.591	0.614	0.527	0.627	0.656	0.683	-0.086	0.541	0.551	0.557
CN640037.1	-1.414	0.113	0.133	0.135	-1.394	0.134	0.145	0.154	0.802	0.865	0.889	0.905	-1.259	0.108	0.122	0.131
CN640110.1	0.834	0.713	0.723	0.723	0.433	0.525	0.543	0.570	-2.292	0.043	0.067	0.091	1.320	0.904	0.909	0.917
CN640155.1	-2.474	0.005	0.014	0.026	-2.661	0.005	0.023	0.033	0.396	0.511	0.520	0.542	-1.437	0.026	0.037	0.044
CN640247.1	-1.228	0.136	0.152	0.169	-1.317	0.144	0.168	0.180	-0.459	0.197	0.212	0.219	-0.208	0.491	0.504	0.517
CN640289.1	0.834	0.716	0.738	0.765	1.300	0.946	0.950	0.976	0.571	0.750	0.765	0.785	0.724	0.783	0.785	0.792
CN640361.1	1.188	0.915	0.934	0.957	1.503	0.945	0.962	0.969	0.974	0.955	0.967	0.979	0.182	0.653	0.664	0.669
CN640419.1	1.118	0.875	0.895	0.910	1.438	0.949	0.966	0.984	0.018	0.300	0.321	0.333	0.993	0.849	0.854	0.866
CN640485.1	-1.201	0.132	0.157	0.167	-1.203	0.154	0.161	0.173	0.470	0.576	0.601	0.616	-0.847	0.231	0.245	0.251
CN640493.1	-0.111	0.407	0.408	0.424	-0.242	0.411	0.423	0.445	0.693	0.846	0.875	0.884	-0.896	0.166	0.173	0.175
CN640521.1	0.497	0.633	0.635	0.650	0.652	0.705	0.717	0.741	0.748	0.867	0.890	0.905	-0.170	0.506	0.519	0.522
CN640670.1	na	na	na	na	na	na	na	na	na	na	na	na	na	na	na	na
CN640738.1	0.335	0.622	0.639	0.656	0.477	0.674	0.696	0.720	-0.617	0.169	0.182	0.183	1.040	0.882	0.889	0.895
CN641116.1	-0.099	0.450	0.467	0.473	-0.185	0.434	0.448	0.460	0.496	0.602	0.610	0.635	-0.700	0.301	0.301	0.308
CN641171.1	1.297	0.934	0.950	0.967	0.918	0.790	0.800	0.804	0.824	0.920	0.924	0.935	-1.065	0.138	0.152	0.160
CN641226.1	0.991	0.824	0.833	0.850	1.228	0.906	0.917	0.917	-0.197	0.231	0.255	0.276	0.955	0.843	0.850	0.863

ES418315.1	0.619	0.739	0.762	0.768	0.680	0.751	0.762	0.789	-0.623	0.174	0.183	0.189	0.982	0.868	0.882	0.887
ES418915.1	0.086	0.464	0.465	0.494	0.112	0.504	0.528	0.542	-0.199	0.243	0.245	0.248	0.251	0.662	0.669	0.670
ES419198.1	-1.091	0.155	0.172	0.202	-0.803	0.247	0.249	0.263	0.513	0.624	0.635	0.644	-0.232	0.482	0.494	0.496
ES419223.1	-0.318	0.359	0.388	0.401	0.077	0.516	0.539	0.549	-0.039	0.311	0.334	0.345	0.742	0.808	0.810	0.818
ES419242.1	0.657	0.419	0.421	0.430	0.442	0.426	0.449	0.470	0.462	0.586	0.590	0.614	-0.636	0.326	0.337	0.343
ES419657.1	0.610	0.379	0.403	0.413	0.576	0.564	0.584	0.599	0.571	0.785	0.803	0.819	-0.341	0.481	0.487	0.489
ES420171.1	-1.447	0.121	0.150	0.176	-1.789	0.061	0.077	0.085	-2.066	0.046	0.072	0.094	0.577	0.764	0.771	0.773
ES420250.1	-2.339	0.021	0.045	0.055	-2.448	0.024	0.041	0.051	-1.261	0.086	0.087	0.111	0.070	0.617	0.630	0.641
ES420603.1	-1.848	0.047	0.054	0.070	-2.237	0.033	0.047	0.056	0.127	0.375	0.387	0.412	-1.641	0.029	0.035	0.036
ES420757.1	-1.357	0.130	0.149	0.163	-1.280	0.177	0.203	0.210	0.170	0.329	0.340	0.352	-0.395	0.446	0.455	0.458
ES420771.1	-2.260	0.019	0.043	0.069	-2.266	0.042	0.069	0.098	0.227	0.383	0.387	0.400	-0.937	0.181	0.184	0.185
ES420862.1	-0.526	0.296	0.311	0.331	-0.125	0.454	0.484	0.508	-0.512	0.193	0.199	0.216	1.131	0.898	0.909	0.914
ES421219.1	1.232	0.918	0.947	0.968	0.912	0.812	0.827	0.829	0.931	0.939	0.952	0.962	-1.090	0.155	0.169	0.172
ES421311.1	-1.448	0.086	0.102	0.108	-1.813	0.071	0.082	0.103	0.577	0.681	0.698	0.720	-1.760	0.006	0.007	0.016
ES421603.1	-2.943	0.004	0.015	0.024	-3.168	0.003	0.008	0.026	0.447	0.553	0.565	0.579	-1.874	0.002	0.006	0.015
ES421877.1	-0.168	0.369	0.391	0.394	0.160	0.493	0.518	0.528	0.249	0.432	0.437	0.466	0.406	0.701	0.709	0.713
ES422367.1	-1.149	0.157	0.176	0.194	-1.170	0.184	0.196	0.201	-0.113	0.293	0.301	0.320	-0.360	0.453	0.461	0.464
ES424016.1	-0.295	0.363	0.392	0.417	-0.164	0.440	0.461	0.471	1.029	0.985	0.996	0.999	-0.771	0.264	0.267	0.273
ES428620.1	-0.921	0.199	0.224	0.252	-0.940	0.225	0.252	0.267	-0.974	0.120	0.142	0.171	0.552	0.760	0.762	0.775
Pm_CL135Contig1	0.005	0.519	0.548	0.563	0.068	0.553	0.576	0.602	0.261	0.450	0.474	0.484	-0.120	0.531	0.542	0.553
Pm_CL1400Contig1	1.473	0.963	0.990	1.000	1.880	0.983	0.990	0.995	-0.632	0.166	0.191	0.211	1.936	0.970	0.977	0.991
Pm_CL150Contig1	0.891	0.753	0.756	0.762	0.810	0.703	0.726	0.740	0.717	0.908	0.915	0.918	-0.525	0.403	0.418	0.425
Pm_CL1692Contig1	-0.143	0.435	0.452	0.480	0.117	0.532	0.540	0.563	0.612	0.703	0.726	0.741	-0.073	0.547	0.557	0.565
Pm_CL1811Contig1	0.007	0.495	0.512	0.524	0.146	0.544	0.553	0.577	-1.058	0.115	0.143	0.149	1.306	0.918	0.921	0.932
Pm_CL1814Contig1	1.112	0.876	0.896	0.917	1.124	0.861	0.875	0.897	0.252	0.419	0.422	0.437	0.171	0.638	0.653	0.662
Pm_CL1868Contig1	0.620	0.387	0.395	0.401	0.892	0.767	0.773	0.794	-1.112	0.112	0.140	0.146	1.611	0.917	0.931	0.932
Pm_CL1982Contig1	na	na	na	na	na	na	na	na	na	na	na	na	na	na	na	na
Pm_CL1994Contig1	-0.968	0.191	0.214	0.224	-0.815	0.252	0.260	0.273	-0.287	0.242	0.261	0.273	0.223	0.666	0.671	0.680
Pm_CL1997Contig1	-0.537	0.303	0.306	0.319	-0.824	0.250	0.276	0.302	-0.634	0.169	0.194	0.201	-0.212	0.512	0.527	0.531
Pm_CL1Contig2	1.532	0.974	0.980	0.984	1.546	0.948	0.976	0.993	0.469	0.580	0.604	0.630	0.110	0.631	0.636	0.638
Pm_CL2089Contig1	0.610	0.375	0.384	0.401	0.318	0.378	0.408	0.429	-3.798	0.009	0.012	0.015	2.617	0.988	0.994	0.999
Pm_CL2133Contig1	0.991	0.821	0.847	0.859	0.927	0.773	0.795	0.816	0.886	0.978	0.995	0.999	-0.555	0.386	0.396	0.400

Pm_CL214Contig1	-0.557	0.294	0.307	0.316	-0.435	0.351	0.360	0.387	-1.273	0.094	0.118	0.127	1.171	0.889	0.892	0.903
Pm_CL2282Contig1	0.610	0.394	0.403	0.411	1.001	0.893	0.905	0.926	0.105	0.239	0.242	0.251	0.877	0.810	0.814	0.823
Pm_CL234Contig1	1.499	0.970	0.979	0.983	1.717	0.971	0.985	0.999	-2.352	0.025	0.032	0.054	3.149	0.998	1.000	1.000
Pm_CL618Contig1	na	na	na	na	na	na	na	na	na	na	na	na	na	na	na	na
Pm_CL61Contig1	0.343	0.558	0.577	0.605	0.543	0.641	0.662	0.673	-1.594	0.068	0.069	0.072	1.909	0.965	0.978	0.990
Pm_CL73Contig1	0.615	0.706	0.727	0.729	0.911	0.808	0.810	0.822	0.517	0.610	0.621	0.646	0.361	0.708	0.710	0.711
Pm_CL783Contig1	1.565	0.979	0.984	0.992	1.639	0.961	0.979	0.990	0.935	0.953	0.959	0.989	-0.143	0.519	0.523	0.529
Pm_CL795Contig1	-0.705	0.214	0.242	0.257	-0.800	0.258	0.285	0.314	-1.676	0.070	0.086	0.115	0.962	0.834	0.848	0.854
Pm_CL855Contig1	-1.965	0.042	0.049	0.052	-2.053	0.052	0.058	0.068	0.520	0.655	0.672	0.678	-1.258	0.062	0.063	0.072
Pm_CL908Contig1	0.853	0.813	0.822	0.849	-0.119	0.456	0.481	0.497	-7.346	<0.001	na	na	5.302	1.000	1.000	1.000
Pm_CL919Contig1	0.240	0.574	0.580	0.596	0.245	0.592	0.611	0.615	-0.479	0.196	0.221	0.224	0.572	0.778	0.782	0.790
Pm_CL922Contig1	-2.224	0.009	0.020	0.043	-2.367	0.009	0.033	0.055	0.277	0.421	0.442	0.455	-1.186	0.069	0.082	0.083
Pm_CL939Contig1	0.978	0.825	0.845	0.866	0.713	0.732	0.741	0.744	0.942	0.957	0.960	0.973	-1.076	0.150	0.154	0.158
Pm_CL969Contig1	-1.469	0.098	0.122	0.129	-1.485	0.129	0.132	0.140	0.501	0.630	0.642	0.666	-0.954	0.181	0.193	0.200
Pm_CL988Contig1	0.497	0.622	0.626	0.633	0.102	0.516	0.523	0.525	-0.605	0.177	0.203	0.211	-0.109	0.542	0.548	0.558
sM13Df243	-0.217	0.388	0.405	0.422	-0.136	0.450	0.468	0.489	0.185	0.385	0.398	0.426	-0.067	0.550	0.563	0.570
sSPcDFD005F06506	-1.480	0.085	0.108	0.128	-1.676	0.089	0.110	0.132	-0.561	0.183	0.207	0.227	-0.412	0.418	0.432	0.442
sSPcDFD015C12212	na	na	na	na	na	na	na	na	na	na	na	na	na	na	na	na
sSPcDFD024D11311	-1.965	0.040	0.068	0.080	-2.053	0.049	0.078	0.078	0.520	0.650	0.657	0.659	-1.258	0.056	0.058	0.058
sSPcDFD040B03103	0.509	0.625	0.647	0.666	0.020	0.484	0.495	0.523	0.705	0.822	0.834	0.845	-1.451	0.033	0.047	0.047
sSPcDFE002A03003	-1.055	0.166	0.179	0.188	-1.074	0.207	0.232	0.249	-0.120	0.299	0.318	0.332	-0.243	0.471	0.482	0.485
sSPcDFE025C06206	1.678	0.987	0.994	0.999	1.463	0.929	0.945	0.947	-1.807	0.049	0.055	0.064	1.849	0.974	0.977	0.991
sSPcDFE028B10110	-0.523	0.312	0.313	0.322	-0.676	0.283	0.311	0.333	0.868	0.930	0.957	0.961	-1.279	0.084	0.094	0.107
sSPcDFE038D06306	-1.201	0.142	0.147	0.149	-1.435	0.129	0.132	0.137	0.675	0.772	0.772	0.783	-1.507	0.037	0.048	0.062
sSPcDFE044F10510	-1.091	0.150	0.173	0.173	-1.316	0.147	0.162	0.164	-1.316	0.089	0.108	0.111	0.322	0.686	0.691	0.693
sSPcDFE049B06106	-1.612	0.031	0.045	0.073	-1.729	0.034	0.050	0.065	0.216	0.264	0.270	0.288	-0.870	0.272	0.282	0.292
sSPcDFE049E11411	0.128	0.469	0.481	0.482	0.094	0.491	0.508	0.516	0.860	0.958	0.974	1.000	-0.770	0.263	0.272	0.284
sSPcDFF014F08508	0.930	0.756	0.782	0.797	0.713	0.611	0.613	0.634	0.691	0.875	0.890	0.911	-0.800	0.279	0.282	0.285
sSPcDFF015H05705	-1.285	0.129	0.129	0.151	-1.235	0.160	0.166	0.182	0.776	0.860	0.862	0.891	-1.070	0.152	0.164	0.176
sSPcDFF044H10710	0.398	0.620	0.634	0.640	0.438	0.639	0.664	0.682	-0.081	0.296	0.312	0.316	0.292	0.681	0.692	0.701
U22458.1	na	na	na	na	na	na	na	na	na	na	na	na	na	na	na	na
Z49715.1	-0.268	0.395	0.421	0.443	-0.142	0.450	0.473	0.479	-0.777	0.150	0.151	0.155	0.949	0.870	0.870	0.872

| Average | -0.170 | -0.194 | -0.106 | -0.012 |
| SD | 1.117 | 1.194 | 1.131 | 1.189 |

Probability values (*P*) corresponding to the left tail of the null distribution were derived from 10,000 coalescent simulations assuming a Wright-Fisher population (WF), an instantaneous growth model (IGM) and a bottleneck model with the timing of the bottleneck set at 100,000 yrs ago (BIM_100). D_{fl} = Fu and Li's *D* (FU AND LI 1993), *E* = Zeng *et al.*'s *E* (ZENG *et al.* 2006), *F* = Fu and Li's *F* (FU AND LI 1993), *H* = normalized value of Fay and Wu's *H* (FAY AND WU 2000; ZENG *et al.* 2006) and SD = standard deviation.

TABLE S10

Results from a maximum-likelihood ratio test for the presence of selective sweeps using a HKA test

	$\log L$	χ^2	P	k_1	k_2	k_3
Null model	-92.15	---	---	1.00	1.00	1.00
Alternative model	-85.85	12.60	0.006	0.32	0.58	0.41
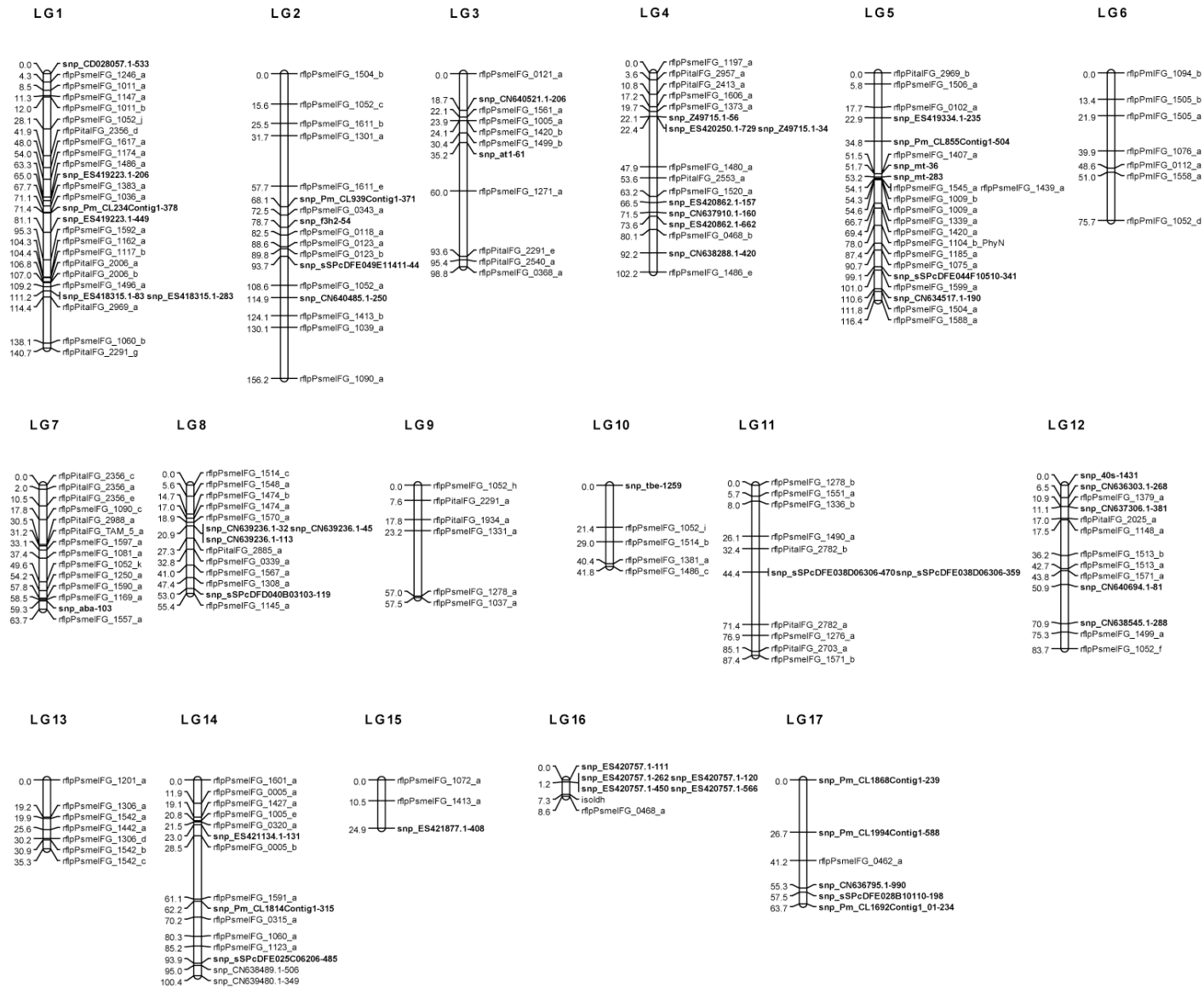
FIGURE S1.—An illustration of the Douglas-fir linkage map. SNP markers located within the same candidate gene were removed if they had similar patterns of segregation or were located within 0.5 cM of each other (*n* = 10). Illustrated are 54 SNPs from 42 unique candidate genes.
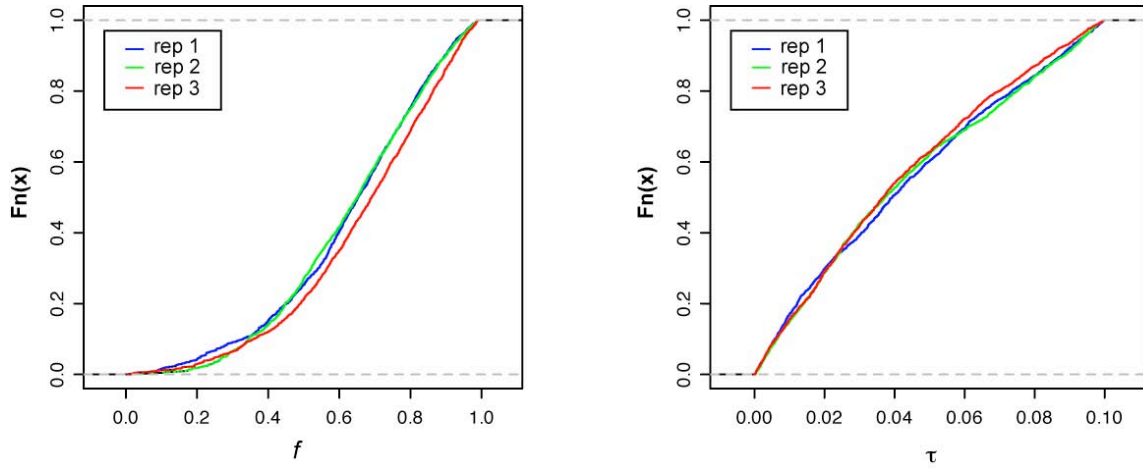
FIGURE S2.—Cumulative distribution plots for the parameters under the instantaneous growth model. Separate runs of the MCMC sampler are differentiated using color.
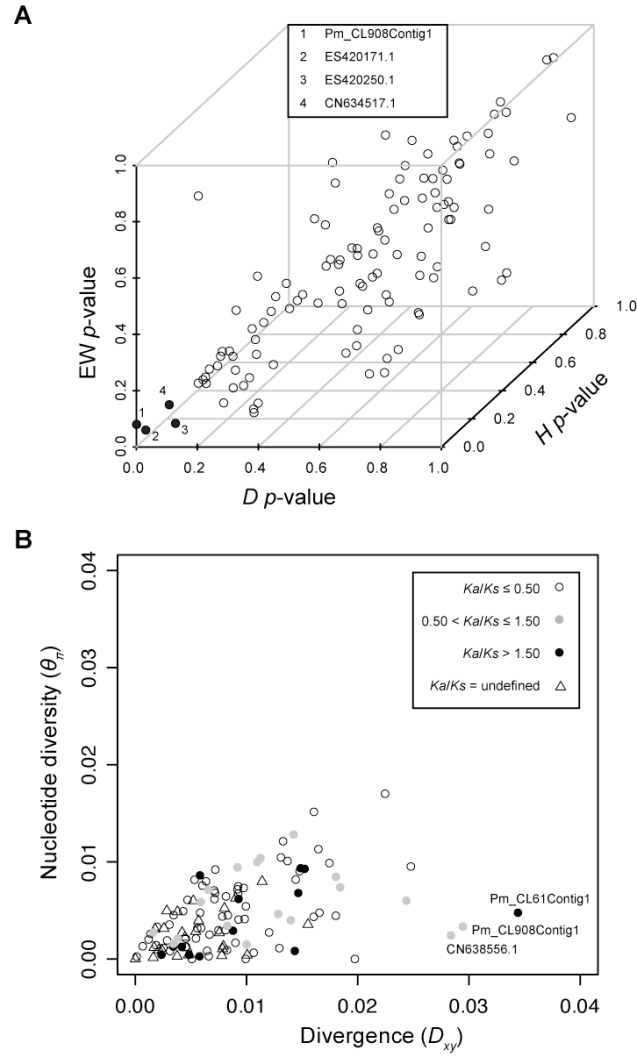
FIGURE S3.—Patterns of neutrality and polymorphism-to-divergence across 121 candidate genes putatively affecting cold-tolerance in coastal Douglas fir. (A) An illustration of the compound *DHEW* test for positive selection. (B) Patterns of polymorphism-to-divergence using all sites. Estimates of diversity and divergence are scaled by the length of the alignment for each candidate gene. Labeled are those candidate genes exhibiting an excess of divergence relative to polymorphism as detected using a HKA test (cf. Materials and Methods). Colors and shapes of the points relate overall patterns of diversity and divergence to the ratio of nonsynonymous to synonymous divergence.
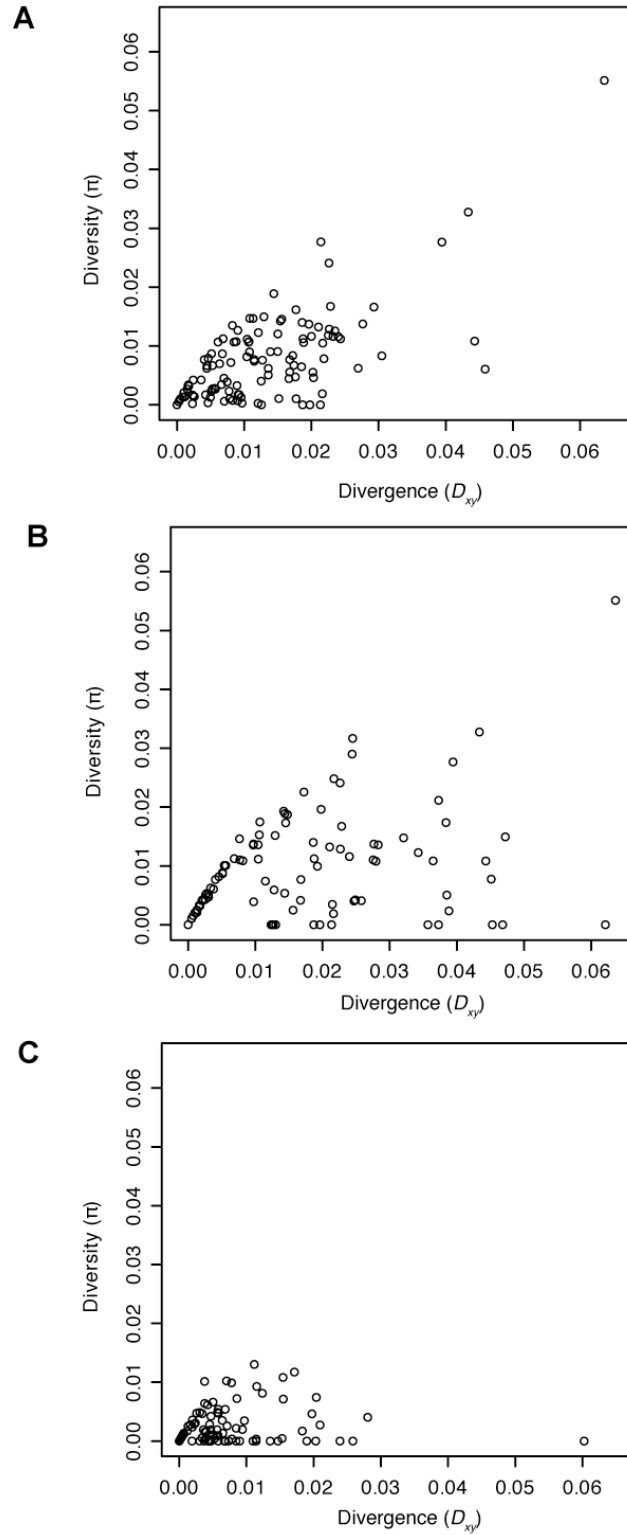
FIGURE S4.—Diversity and divergence across different categories of sites – (A) silent sites, (B) synonymous sites and (C) nonsynonymous sites. All estimates are scaled to the number of sites within each category.
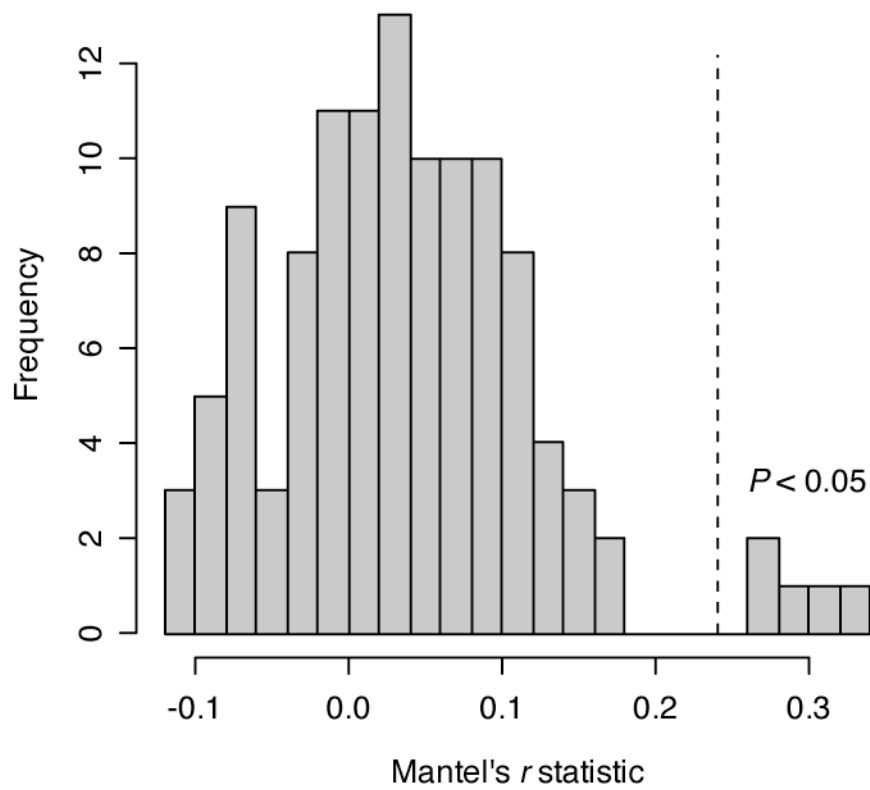
FIGURE S5.—The distribution of Mantel's *r* statistic for the 115 polymorphic candidate genes. These statistics describe the correlation between among population divergence (D_{xy}) and distance (km) for each candidate gene. The dashed lines separates those values significant at *P* = 0.05.
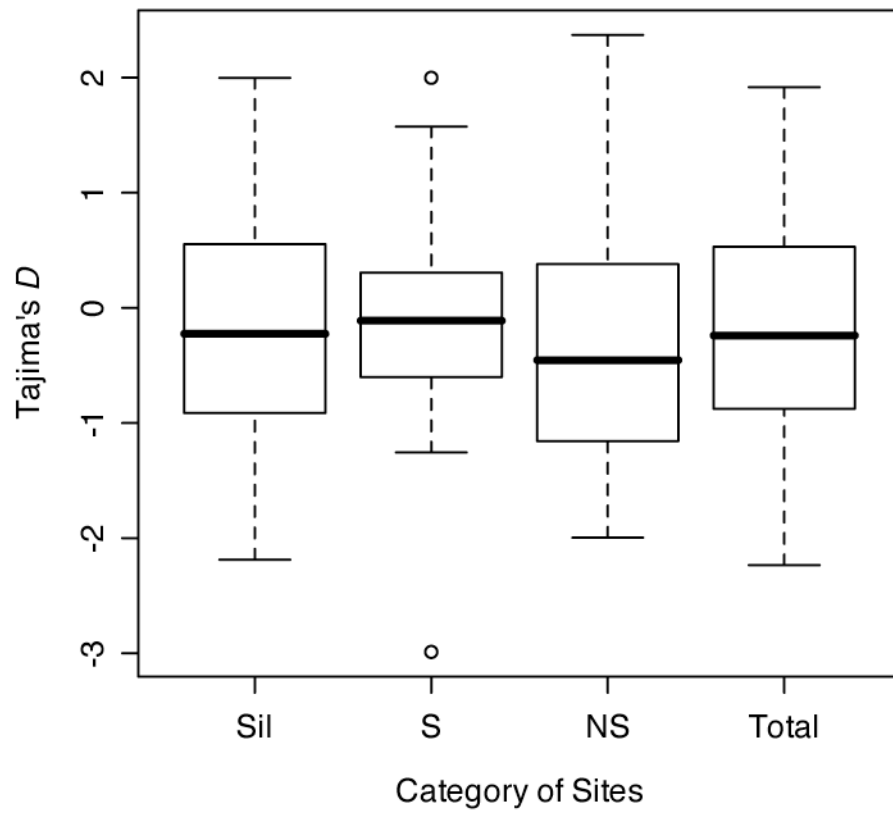
FIGURE S6.—Distribution of Tajima's *D* across different categories of sites. S, synonymous sites; Sil, silent sites; NS, nonsynonymous sites; Total, all sites.

REFERENCES

FAY, J. C. AND C.-I. WU, 2000 Hitchhiking under positive Darwinian selection. Genetics **155:** 1405–1413.

FU, Y.-X. AND W.-H. LI, 1993 Statistical tests of neutrality of mutations. Genetics **133:** 693–709.

NEI, M. AND T. GOJOBORI, 1986 Simple methods for estimating the numbers of synonymous and nonsynonymous nucleotide substitutions. Mol. Biol. Evol. **3:** 418–426.

TAJIMA, F., 1989 Statistical method for testing the neutral mutation hypothesis by DNA polymorphism. Genetics **123:** 585–595.

WATTERSON, G., 1978 The homozygosity test of neutrality. Genetics **88:** 405–417.

ZENG, K., Y. X. FU, S. SHI AND C.-I. WU, 2006 Statistical tests for detecting positive selection by utilizing high-frequency variants. Genetics **174:** 1431–1439.